Integration of Network Pharmacology and Molecular Docking Together with an In Vitro Nitric Oxide Inhibition for the Insight for Antipyretic Effects of Benjalokawichian, the Thai Traditional Polyherbal Remedy

Chinnaphat Chaloemram , Ruchilak Rattarom , Anake Kijjoa , Somsak Nualkaew *

Posted Date: 27 February 2026

doi: 10.20944/preprints202602.1199.v1

Keywords: Benjalokawichian; Ha-Rak; toxic fever; network pharmacology; molecular docking; NO inhibition; anti-inflammatory

 doi:10.20944/preprints202602.1199.v1

Article

Integration of Network Pharmacology and Molecular Docking Together with an In Vitro Nitric Oxide Inhibition for the Insight for Antipyretic Effects of Benjalokawichian, the Thai Traditional Polyherbal Remedy

Chinnaphat Chaloemram [1], Ruchilak Rattarom [2], Anake Kijjoa [3] and Somsak Nualkaew [2,*]

[1] Doctor of Philosophy in Pharmacy program, Faculty of Pharmacy, Mahasarakham University, Kantharawichai, Maha Sarakham 44150, Thailand

[2] Pharmaceutical Chemistry and Natural Product Research Unit, Faculty of Pharmacy, Mahasarakham University, Kantharawichai, Maha Sarakham 44150, Thailand

[3] School of Medicine and Biomedical Sciences Abel Salazar (ICBAS) and CIIMAR, Universidade do Porto, Rua de Jorge Viterbo Ferreira 228, 4050-313 Porto, Portugal

* Correspondence: somsak.n@msu.ac.th (S.N.); Tel.: +6685-137-6763

Abstract

Benjalokawichian (BLW) or Ha-Rak is a classic antipyretic polyherbal remedy used in Thai traditional medicine (TTM) to reduce toxic fever (TF). This study aimed to shed light to the mechanisms of action and identify bioactive components of BLW responsible for TF treatment. The approaches that integrate network pharmacology, molecular docking, and inhibition of nitric oxide (NO) production in LPS-induced RAW264.7 were used for these purposes. Network pharmacology was used as a tool to identify 17 potential bioactive compounds, 88 potential therapeutic targets, and 4 hub genes for BLW. Among the key targets, TNF, PTGS2, STAT3, and NFKB1 were closely associated with the phenylalanine, arachidonic acid and tyrosine metabolic pathways, which play critical roles in infections, inflammation, proliferation and apoptosis in the TF microenvironment. On the other hand, molecular docking analysis suggested that core compounds exhibited strong binding affinities for key targets, with binding energies ranging from -4.5 to -11.1 kJ/mol. In vitro assay showed that BLW extract exhibited strong inhibition of NO production in LPS-induced RAW264.7 macrophages, with an IC_{50} value of 69.10 μg/mL, and no cytotoxicity against RAW264.7 macrophages was observed. Furthermore, the biomarker compounds of BLW extract, viz. perforatic acid and peucenin-7-methyl ether were found to decrease NO production in a dose-dependent manner. Overall, this study demonstrates that BLW exerts its therapeutic effects on TF through a complex network of various compounds, targets, and pathways. These findings serve as a foundation for further research into the mechanisms of action of a polyherbal remedy toward TF to provide scientific evidences for its clinical use.

Keywords: Benjalokawichian; Ha-Rak; toxic fever; network pharmacology; molecular docking; NO inhibition; anti-inflammatory

1. Introduction

Fever is recognized as a fundamental host defense mechanism and a hallmark clinical manifestation of inflammatory responses. The febrile process is orchestrated by a complex interplay of endogenous and exogenous pyrogens, and often serves as a primary indicator for numerous pathological states, including microbial infections. These stimuli trigger biosynthesis and systemic release of diverse inflammatory mediators from both immune cells, such as macrophages and

 doi:10.20944/preprints202602.1199.v1

leukocytes, and non-immune lineages like endothelial cells [1–3]. At the molecular level, a critical phase of thermoregulatory adjustment involves the induction of the arachidonic acid metabolic pathway within the preoptic area and anterior hypothalamus (POAH). Specifically, pyrogenic cytokines, most notably interleukin-1β (IL1B), interleukin-6 (IL6), tumor necrosis factor-α (TNF), and interferons (IFNs), upregulate cyclooxygenase-2 (COX-2). This enzymatic activation results in the localized accumulation of prostaglandin E2 (PGE_2), which subsequently resets the hypothalamic thermostat to elevate core body temperature [2–6]. While mild and self-limiting pyrexia generally requires minimal clinical intervention, severe febrile episodes present significant therapeutic challenges and risks. Severe fever is typically characterized by a sustained temperature of 40 °C or higher, or when accompanied by alarming neurological or respiratory symptoms such as nuchal rigidity, intense cephalalgia, or acute dyspnea [7]. Such severe cases often reflect profound systemic inflammation marked by a pathological surge in circulating pro-inflammatory cytokines and chemokines. This dysregulated phenomenon, frequently known as a cytokine storm, can precipitate acute respiratory distress syndrome (ARDS) and multi-organ failure, potentially leading to fatal outcomes if not managed with timely pharmacological intervention [8].

Toxic fever (TF) or severe fever is documented in the Taksila scriptures, which detail the outbreak and treatment of various fevers using principles of Thai traditional medicine (TTM) [9]. Potential signs of TF include a sudden high fever, accompanied by symptoms such as red eyes, cold extremities, headaches, alternating chills and heat, pain, stiff tongue and jaw, labored breathing, dry mouth, drowsiness, unconsciousness, delirium, and rashes appearing on the body, for example scarlet fever, roseola infantum measles, rubel-la, herpes zoster, erysipelas, and typhoid fever [10].

The Thai polyherbal remedy, Benjalokawichian (BLW), frequently referred to as Ha-Rak or the "Five Roots" remedy, is a well-known antipyretic preparation of TTM. Recognized for its therapeutic value, BLW was included in the National List of Herbal Medicinal Products of Thailand in 2006 and remains a standard prescription for the management of febrile illnesses. According to the Taksila scriptures, this traditional remedy is specifically indicated for alleviating toxic fever associated with inflammatory pathologies as well as for treatment of inflammatory and allergic dermatological conditions. BLW consists of equal proportions of roots of five plants, i. e. *Capparis micracantha* DC., *Clerodendrum indicum* (L.) Kuntze, *Ficus racemosa* L., *Harrisonia perforata* (Blanco) Merr., and *Tiliacora triandra* (Colebr.) Diels [11,12]. The conventional preparation of BLW involves boiling a mixture of equal amounts of small pieces (1-2 cm in length) of air-dried roots of the five plants with water (1:5 w/v) in a clay pot for 30 min, cooled to room temperature, and then filtered with a cheesecloth to obtain a decoction. For adult patients, the traditional regimen consists of one glass taken three times per day before meals upon the onset of symptoms. Dosages for pediatric patients are calibrated based on the age of the child [9]. In accordance with the 2023 National List of Essential Herbal Medicines, BLW is also commercially available in modern dosage forms, including powders, tablets, and capsules. The current clinical guidelines suggest a dosage of 1 to 1.5 grams per administration for adults. For children between 6 and 12 years of age, the recommended dose ranges from 0.5 to 1 gram, to be taken three times daily before meals as symptoms persist [13].

Network pharmacology represents a multidimensional methodology that combines bioinformatics, cheminformatics, and systems biology to elucidate the intricate relationships among bioactive constituents, molecular targets, and disease-related signaling pathways. This strategy has gained more traction in the scientific community for its ability to predict potential binding targets for diverse chemical compounds, establish comprehensive interaction networks involving compounds, targets, and diseases, and pinpoint crucial proteins or hub nodes within complex systems. Consequently, it has become an invaluable tool for investigating the pharmacological profiles of polyherbal formulations and traditional therapeutic systems [14–19].

In continuation of our research project to unravel the mechanisms of action and targets of the bioactive compounds in polyherbal remedies used in TTM, we now describe our study of BLW for the treatment of TF, focusing on its anti-inflammatory actions. The integrated network pharmacology and molecular docking, in combination with pharmacological activity assays, particularly the

 doi:10.20944/preprints202602.1199.v1

inhibition of NO production in LPS-induced RAW264.7 macrophages, were used for these purposes. The results obtained from this study can provide concrete scientific evidence to support the clinical use of this polyherbal remedy.

2. Results

2.1. Screening of Bioactive Compounds and BLW-Related Targets based on ADME

An extensive literature search of the constituents of the five plants belonging to the BLW remedy, *viz. C. micracantha*, *C. indicum*, *F. racemosa*, *H. perforata*, and *T. triandra*, revealed that 32 compounds possess anti-inflammatory activity. However, only 15 compounds satisfied the requirements for drug-likeness and gastrointestinal (GI) absorption criteria, while the remaining 17 compounds with insufficient GI absorption (Supplementary Table S1) were not included. Following this selection, potential protein targets for the eligible compounds were predicted. After removal of redundant entries, a total of 495 unique targets associated with the active compounds were established. Notably, harrisolanol A was the sole compound that exhibited no target prediction probability. Comprehensive details are provided in Supplementary Table S2.

2.2. Obtention of Potential Therapeutic Targets of BLW for Treatment of TF

By using the term "toxic fever" as a search descriptor, a comprehensive set of disease-related targets was collected from various repositories, yielding 8,031 targets from GeneCards, 11 from Online Mendelian Inheritance in Man (OMIM), and 97 from PharmGKB (Supplementary Table S3). To determine the pharmacological intersection, the targets associated with the BLW remedy were compared with those related to TF. This comparative analysis led to the identification of 88 overlapping targets, which were established as the candidate therapeutic target candidates for BLW in managing TF.

2.3. Protein–protein interaction (PPI) Network Visualization and Modular Analysis

The interaction landscape was mapped among the 88 therapeutic target candidates through a PPI network, as shown in Figure 1c. This topological framework comprised 86 nodes, interconnected by 321 edges, and exhibited an average node degree of 7.74 and a local clustering coefficient of 0.245. By applying rigorous topological filtering as shown in Figure 2b-c, four central hub genes were prioritized, i. e. TNF, PTGS2, STAT3, and NFKB1 (Table 1). These hub proteins, which function as key cytokines and enzymes, are integral to the modulation of various biological activities, including signal transduction and oxidoreduction processes. Due to their exceptional network metrics, specifically their high degree, betweenness centrality, and clustering coefficients, these genes were identified as the primary core targets within the global network (Supplementary Table S4). Furthermore, module analysis using the Molecular Complex Detection (MCODE) algorithm revealed ten distinct functional clusters within the network (Figure 3, Table 2). Five of these MCODE-derived modules were further characterized by their unique biological roles. For example, MCODE1 was predominantly associated with arachidonic acid metabolism, ovarian steroidogenesis, and African trypanosomiasis. MCODE2 showed strong correlations with purine and nucleotide metabolism as well as morphine addiction. MCODE3 was linked to the metabolic pathways of amino acids, specifically phenylalanine, tyrosine, and histidine. Finally, MCODE4 was involved in the calcium signaling pathway and neuroactive ligand-receptor interactions, as detailed in Table 2.

 doi:10.20944/preprints202602.1199.v1

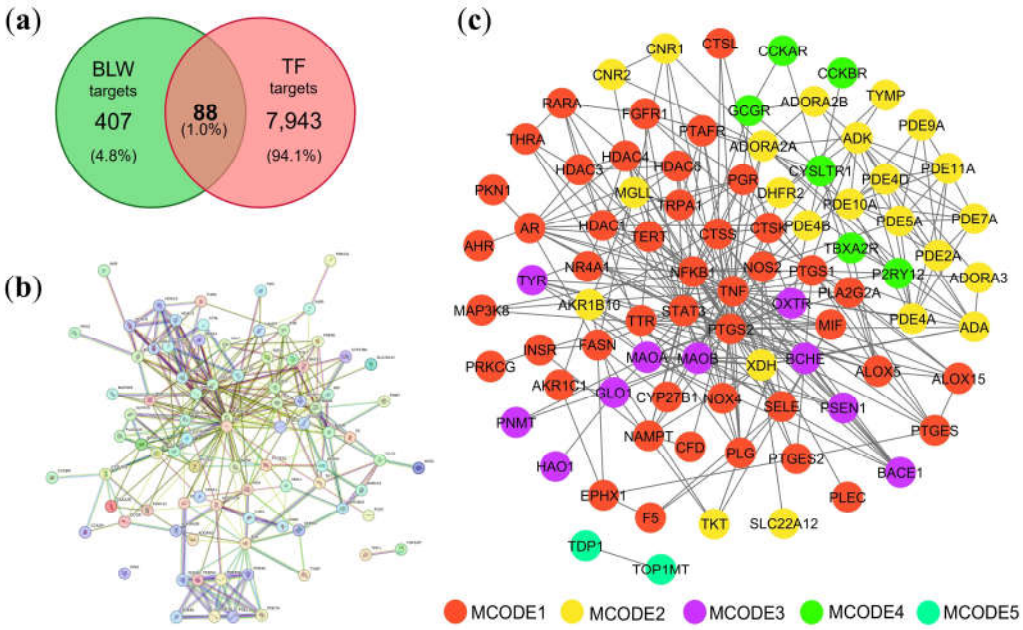

Figure 1. Network pharmacological analysis of overlapping genes between BLW and TF-related targets. (**a**) Venn diagram illustrating the intersection of targets; (**b**) Protein–protein interaction (PPI) network constructed using the STRING database; (**c**) Network topology analysis performed with Cytoscape. Circles of different colors represent distinct MCODE clusters.

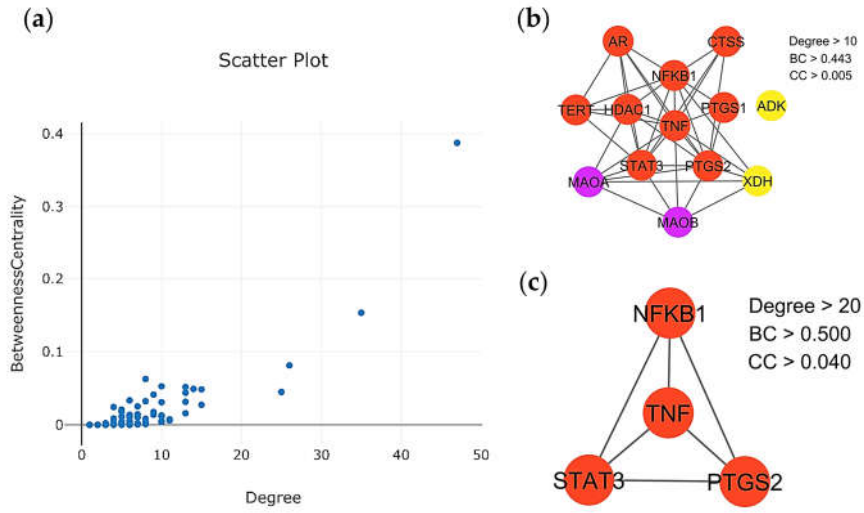

Figure 2. Screening process for hub genes in the PPI network. (**a**) Scatter plot showing the distribution of degree values; (**b**) Identification of genes with a degree >10; (**c**) Identified four hub genes. Circles with different colors represent different MCODE clusters.

Table 1. Descriptions of the PPI network hub genes.

Target	Degree	Betweenness centrality	Closeness centrality	Type
TNF	47	0.669354	0.387608	Cytokines
PTGS2	35	0.588652	0.153506	Oxidoreductase
STAT3	26	0.532051	0.081417	Transcription
NFKB1	25	0.515527	0.044900	Transcription

 doi:10.20944/preprints202602.1199.v1

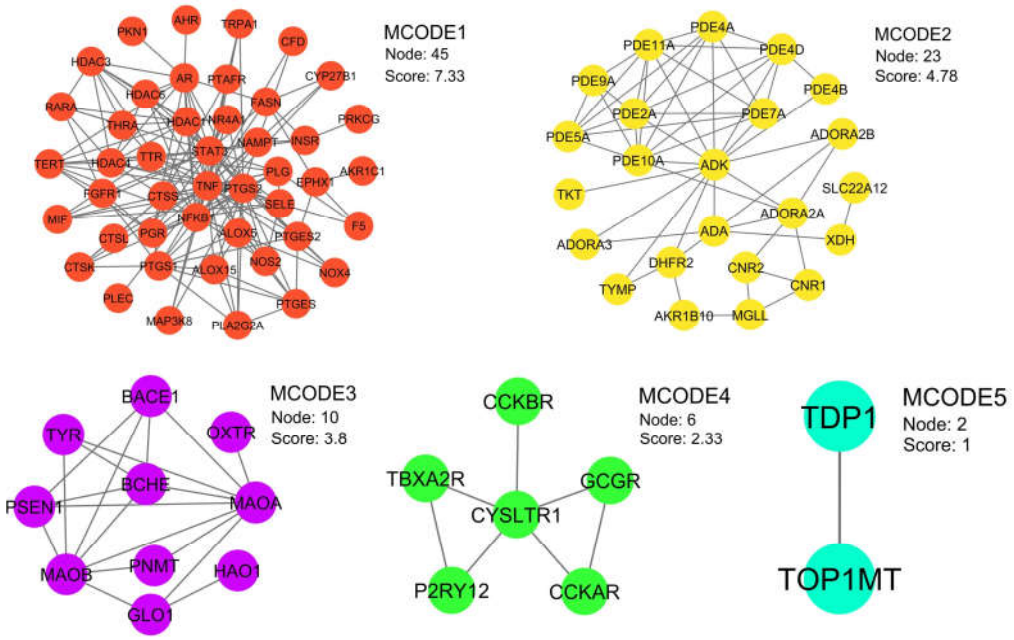

Figure 3. Application of gene ontology (GO) enrichment analysis to MCODE module analysis for sub-network categorization and different MCODE networks are presented with different colors.

Table 2. The results of MCODE enrichment analysis.

MCODE	Pathway	Description	Fold enrichment
MCODE1	hsa00590	Arachidonic acid metabolism	22.6
MCODE1	hsa05143	African trypanosomiasis	16.0
MCODE1	hsa04913	Ovarian steroidogenesis	11.6
MCODE2	hsa00230	Purine metabolism	36.9
MCODE2	hsa05032	Morphine addiction	30.3
MCODE2	hsa01232	Nucleotide metabolism	18.5
MCODE3	hsa00360	Phenylalanine metabolism	120.3
MCODE3	hsa00350	Tyrosine metabolism	106.9
MCODE3	hsa00340	Histidine metabolism	87.5
MCODE4	hsa04020	Calcium signaling pathway	22.8
MCODE4	hsa04080	Neuroactive ligand-receptor interaction	19.7

2.4. Gene Ontology (GO) and Enriched Pathway Analysis

The enrichment analysis results revealed a total of 19 significant signaling pathways within the KEGG (Kyoto Encyclopedia of Genes and Genomes) database. Furthermore, GO analysis identified 133 biological process (BP) terms, 23 molecular function (MF) terms, and 38 cellular component (CC) terms, all of which are detailed in Supplementary Table S5. The signaling pathways are visualized in the bubble plot in Figure 4, while Figure 5 illustrates the top 10 GO terms across the BP, MF, and CC categories. In these plots, the bubble dimensions correspond to the count of enriched genes, and the color intensity reflects the *p*-values. Specifically, darker shades represent higher statistical significance with smaller *p*-values, and larger bubbles indicate a greater number of enriched therapeutic genes, suggesting a more robust association with the treatment of TF. According to the KEGG pathway enrichment findings, the most significantly enriched pathways included phenylalanine metabolism, arachidonic acid metabolism, and tyrosine metabolism. These pathways were prominently featured within the KEGG pathway network as shown in Figure 4. Additionally,

 doi:10.20944/preprints202602.1199.v1

Figure 6 highlights the arachidonic acid metabolism signaling pathway, specifically identifying potential targets involved in the condition.

In the BP category, the three most significant terms identified were the negative regulation of cardiac muscle relaxation, the negative regulation of calcidiol 1-monooxygenase activity, and the positive regulation of leukocyte adhesion to arterial endothelial cells. For the MF category, significant enrichment was observed in prostaglandin-endoperoxide synthase (PTGS) activity, aliphatic amine oxidase activity, and G-protein coupled adenosine receptor activity. Regarding the CC category, the endolysosome lumen, nuclear envelope lumen, and histone deacetylase complex emerged as the most enriched terms.

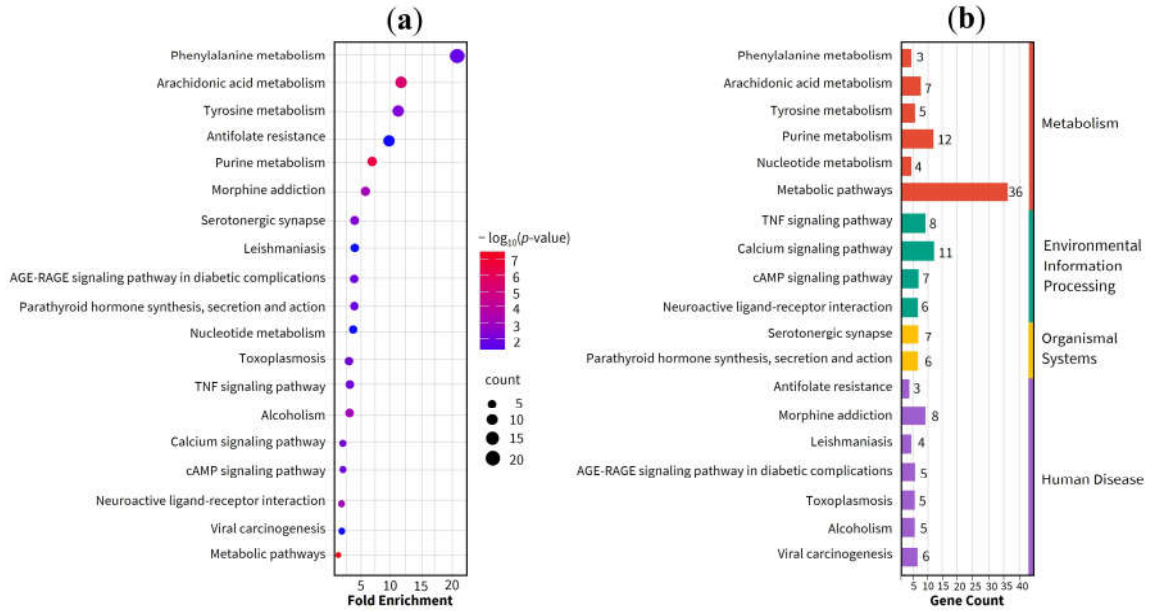

Figure 4. KEGG pathway enrichment analysis. (**a**) The top 30 enriched KEGG pathways based on enrichment score. (**b**) Classification of KEGG pathways and their corresponding gene counts.

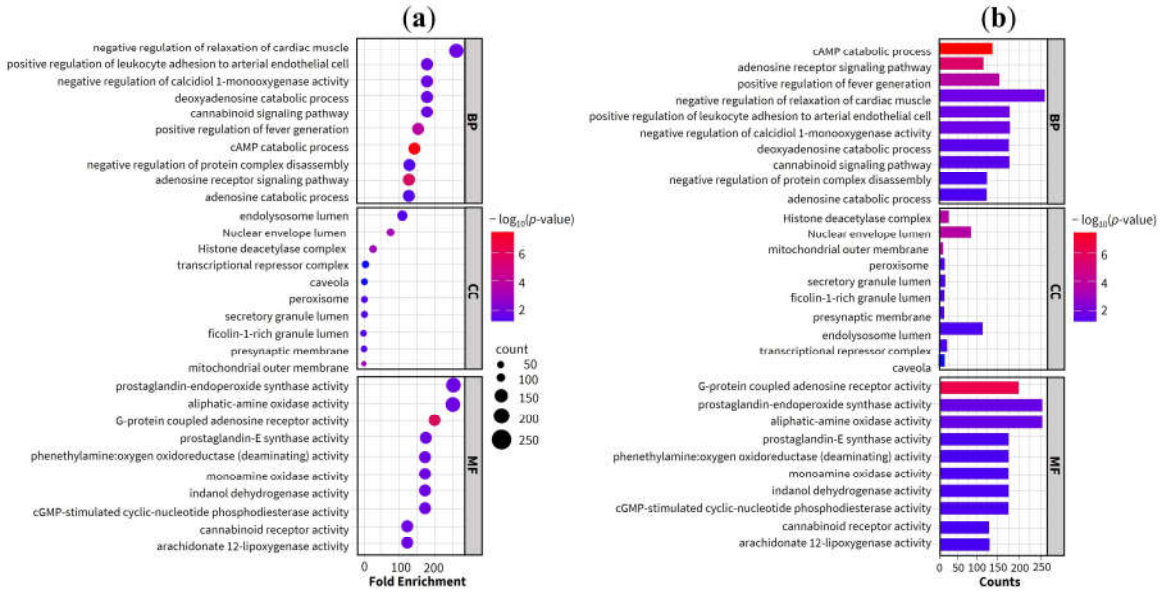

Figure 5. GO enrichment and signaling pathway analysis. (**a**) Bubble plot showing the top 10 enriched terms within the Biological Process (BP), Cellular Component (CC), and Molecular Function (MF) categories. (**b**) Bar plot illustrates the significantly enriched signaling pathways.

 doi:10.20944/preprints202602.1199.v1

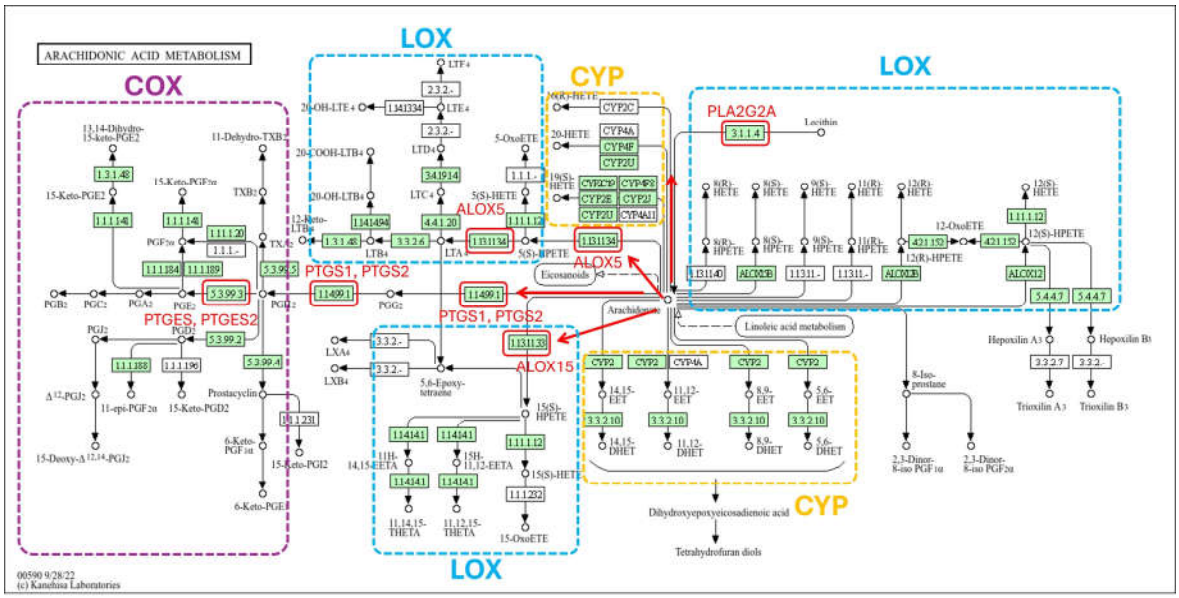

Figure 6. Arachidonic acid metabolism pathway. Red-highlighted boxes represent potential targets of BLW associated with TF. Colored dashed lines demarcate the specific metabolic branches: violet for the cyclooxygenase (COX) pathway, blue for the lipoxygenase (LOX) pathway, and yellow for the cytochrome P450 (CYP) signaling pathway.

2.5. Investigation of the Possible Therapeutic Targets of BLW for TF Treatment

The complex interactions between the identified bioactive constituents and their potential therapeutic targets are shown in Figure 7. This pharmacological network comprised 106 nodes and 189 edges, which collectively represent the binding associations between 14 active compounds and 88 unique targets. Upon analysis of the network topology, specific constituents, including hispidulin and pectolinarigenin of the BLW remedy exhibited the highest degree values (degree = 24).

 doi:10.20944/preprints202602.1199.v1

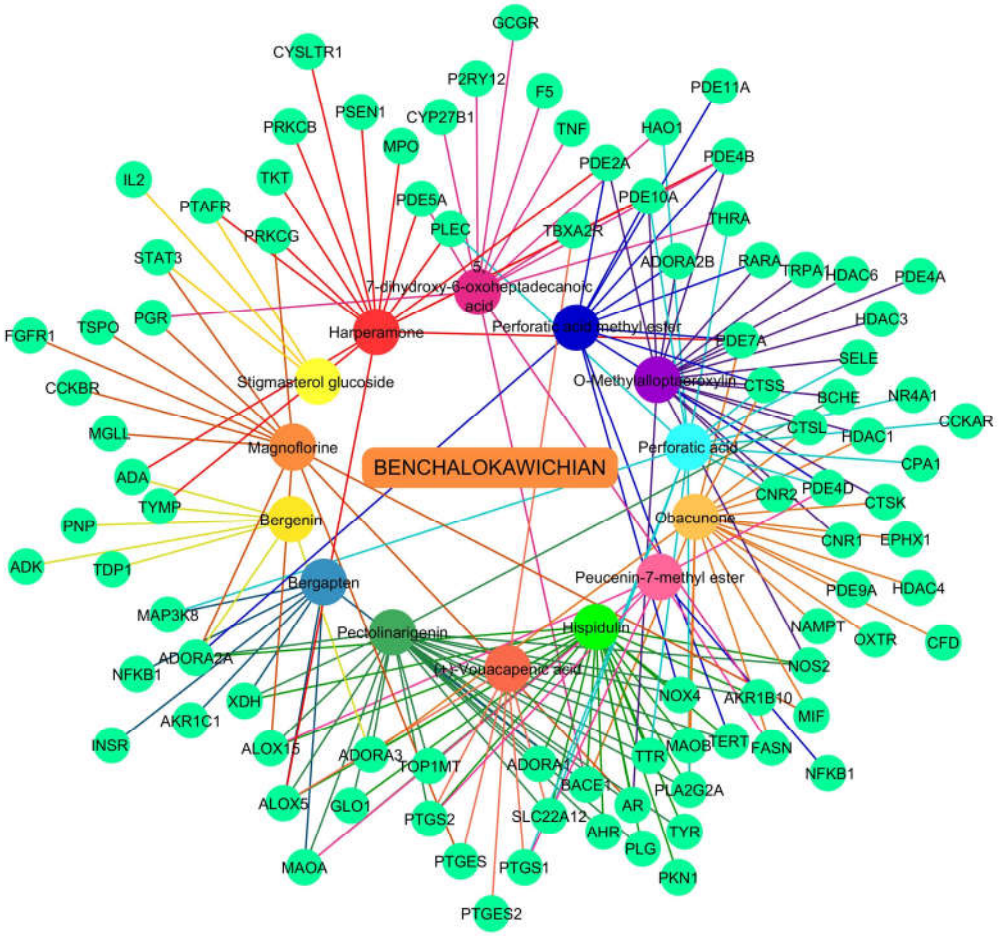

Figure 7. Visualization of the active compounds–potential targets network in the treatment of TF. Green rectangles represent genes associated with TF and targets of the active compounds, while other color circles denote the bioactive compounds of the plants.

2.6. Molecular Docking of Key Targets

The docking simulations evaluated binding affinities for four key targets, *viz*. TNF, PTGS2, STAT3, and NFKB1, with binding energies spanning from -4.5 to -11.1 kJ/mol as shown in Table 3. Analysis of the TNF receptor revealed that obacunone possessed the strongest binding affinity at -9.1 kJ/mol, followed by (+)-vouacapenic acid and stigmasterol glucoside, both at -8.9 kJ/mol, and magnoflorine at -7.9 kJ/mol. In the case of the PTGS2 receptor, hispidulin demonstrated the optimal docking score of -9.4 kJ/mol, followed by perforatic acid methyl ester at -9.3 kJ/mol, while both *O*-methylalloptaeroxylin and perforatic acid recorded values of -8.9 kJ/mol. For the STAT3 receptor, obacunone exhibited the highest affinity at -9.3 kJ/mol, followed by hispidulin and stigmasterol glucoside at -7.7 kJ/mol, and (+)-vouacapenic acid at -7.5 kJ/mol. Furthermore, obacunone showed the most potent interaction with the NFKB1 receptor at -11.1 kJ/mol, surpassing pectolinarigenin at -9.6 kJ/mol, magnoflorine at -9.5 kJ/mol, and hispidulin at -9.3 kJ/mol. Due to the unavailability of the 3D structure for harrisolanol A in the PubChem database, it was excluded from this analysis. Figures 8–11 show the molecular interactions and specific bonding patterns between these active constituents or reference drugs and their target proteins. The characterization of hydrogen bond interactions can be represented through various structural formats, including line, ball-and-stick, and cycle models, to enhance the observation of molecular binding sites. In this study, the specific hydrogen bonding patterns between the target proteins and the ligands are visualized using green dashed line representations. Detailed interaction data and bonding parameters for each protein-ligand complex are shown in Figures 8–11.

 doi:10.20944/preprints202602.1199.v1

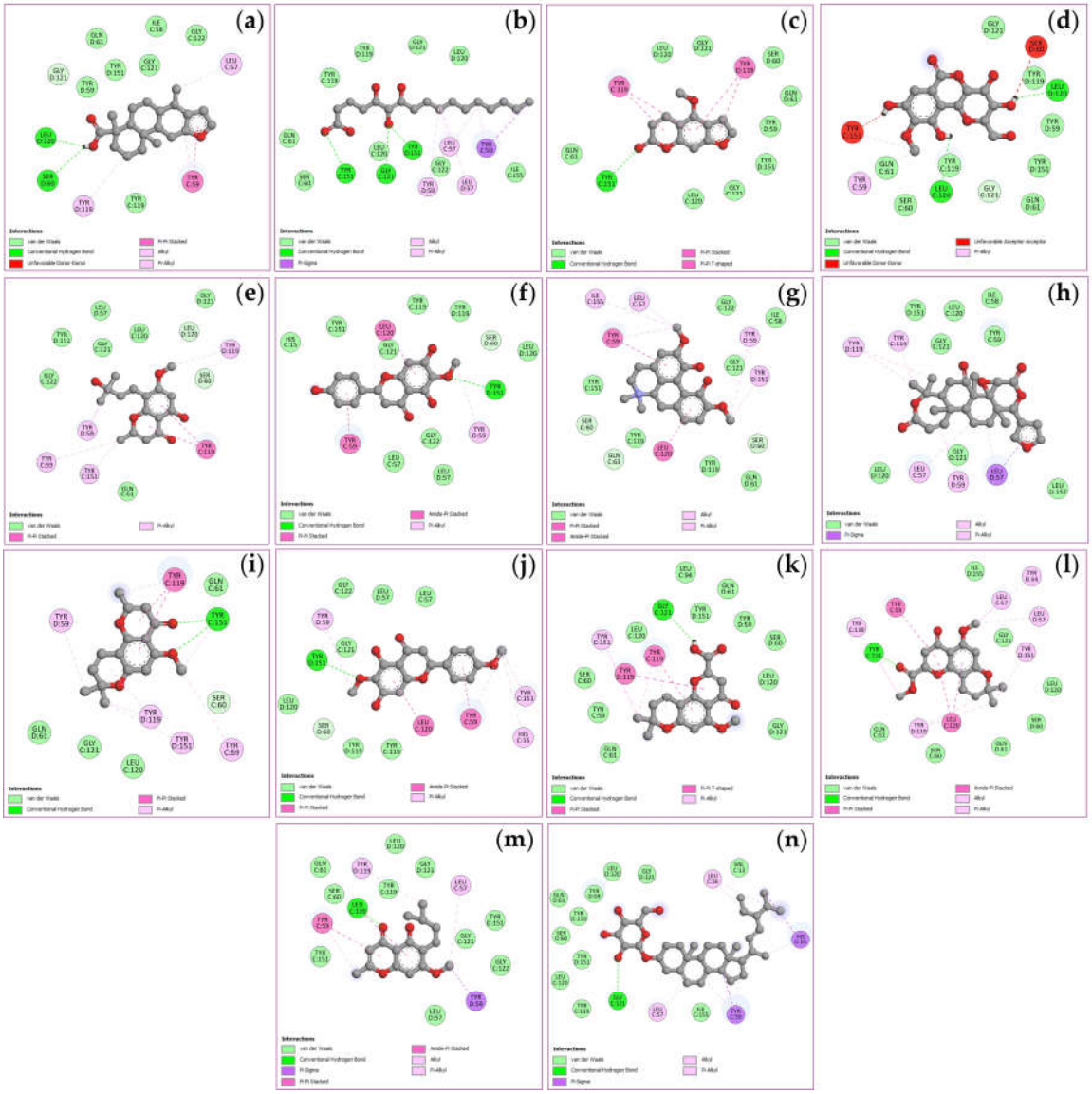

Figure 8. Visualization of molecular docking results for TNF. The molecular docking models depict the interactions between bioactive compounds and TNF: (+)-vouacapenic acid (**a**); 5, 7-dihydroxy-6-oxoheptadecanoic acid (**b**); bergapten (**c**); bergenin (**d**); harperamone (**e**); hispidulin (**f**); magnoflorine (**g**); obacunone (**h**); *O*-methylalloptaeroxylin (**i**); pectolinarigenin (**j**); perforatic acid (**k**); perforatic acid methyl ester (**l**); peucenin-7-methyl ether (**m**); stigmasterol glucoside (**n**).

Table 3. The binding energy of potentially bioactive compounds of BLW and their four target proteins.

Compounds	Binding energy (ΔG_{bind}, kcal/mol)			
	TNF (PDB: 2AZ5)	PTGS2 (PDB: 3LN1)	STAT3 (PDB: 6NJS)	NFKB1 (PDB: 1NFK)
Bioactive compounds				
(+)-Vouacapenic acid	-8.9	-7.8	-7.5	-8.1
5, 7-Dihydroxy-6-oxoheptade canoic acid	-5.1	-6.5	-4.5	-5.1
Bergapten	-6.5	-8.1	-6.0	-7.6
Bergenin	-7.3	-7.2	-7.1	-8.6
Harperamone	-6.6	-8.0	-5.9	-8.0
Hispidulin	-7.4	-9.4	-7.7	-9.3
Magnoflorine	-7.9	-8.8	-7.2	-9.5
Obacunone	-9.1	-8.8	-9.3	-11.1

 doi:10.20944/preprints202602.1199.v1

O-Methylalloptaeroxylin	-7.4	-8.9	-6.9	-8.1
Pectolinarigenin	-7.5	-8.6	-7.1	-9.6
Perforatic acid	-7.5	-8.9	-7.2	-8.5
Perforatic acid methyl ester	-7.4	-9.3	-7.4	-7.9
Peucenin-7-methyl ether	-6.5	-8.3	-6.3	-7.9
Stigmasterol glucoside	-8.9	-8.5	-7.7	-8.5
Standard drug				
Thalidomide	-7.4	-	-	-
Celecoxib	-	-12.1	-	-
Ochromycinone	-	-	-8.3	-
Selinexor	-	-	-	-10.2

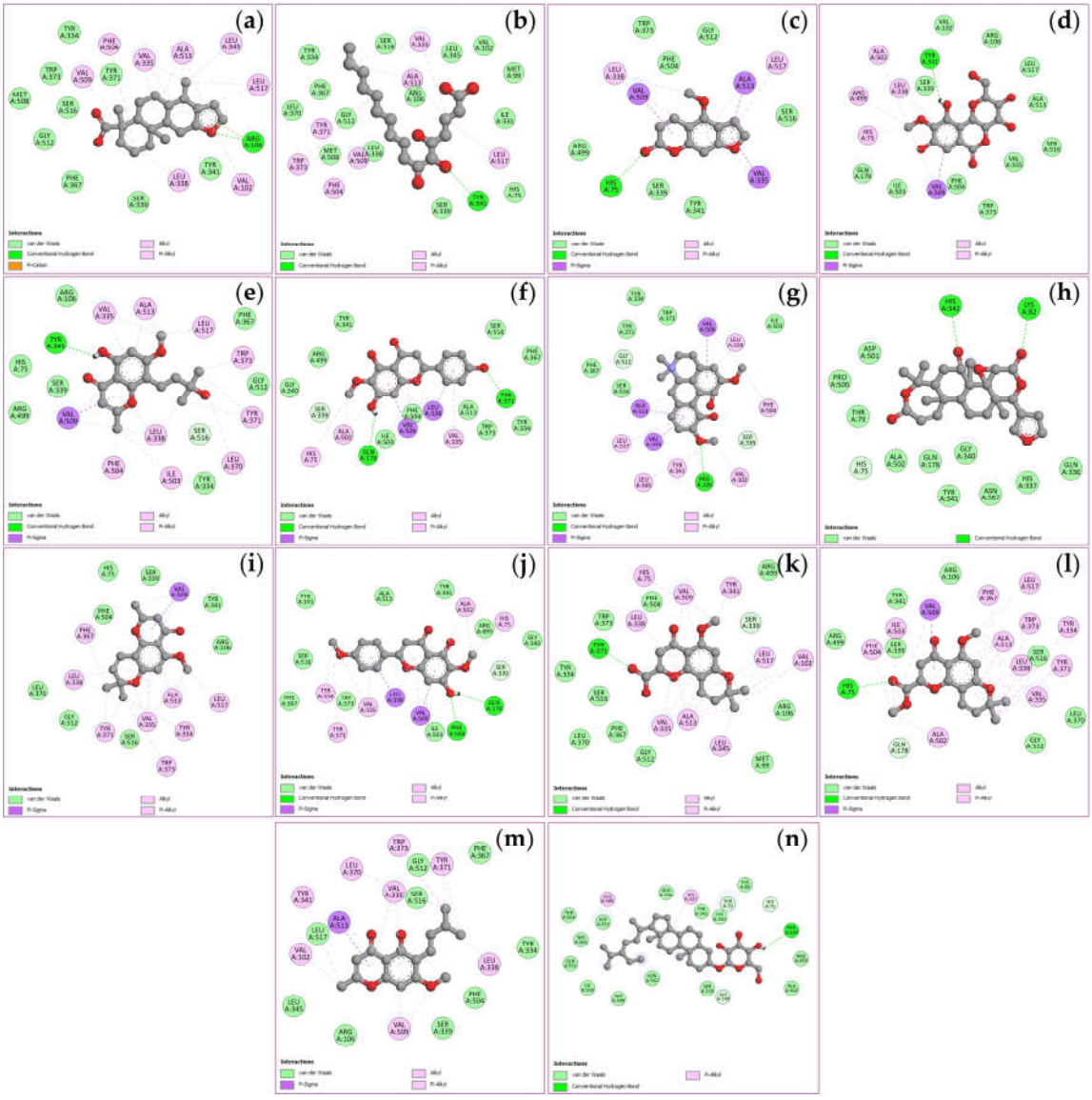

Figure 9. Visualization of molecular docking results for PTGS2. The molecular docking models depict the interactions between bioactive compounds and PTGS2: (+)-vouacapenic acid (**a**); 5, 7-dihydroxy-6-oxoheptadecanoic acid (**b**); bergapten (**c**); bergenin (**d**); harperamone (**e**); hispidulin (**f**); magnoflorine (**g**); obacunone (**h**); *O*-methylalloptaeroxylin (**i**); pectolinarigenin (**j**); perforatic acid (**k**); perforatic acid methyl ester (**l**); peucenin-7-methyl ether (**m**); stigmasterol glucoside (**n**).

 doi:10.20944/preprints202602.1199.v1

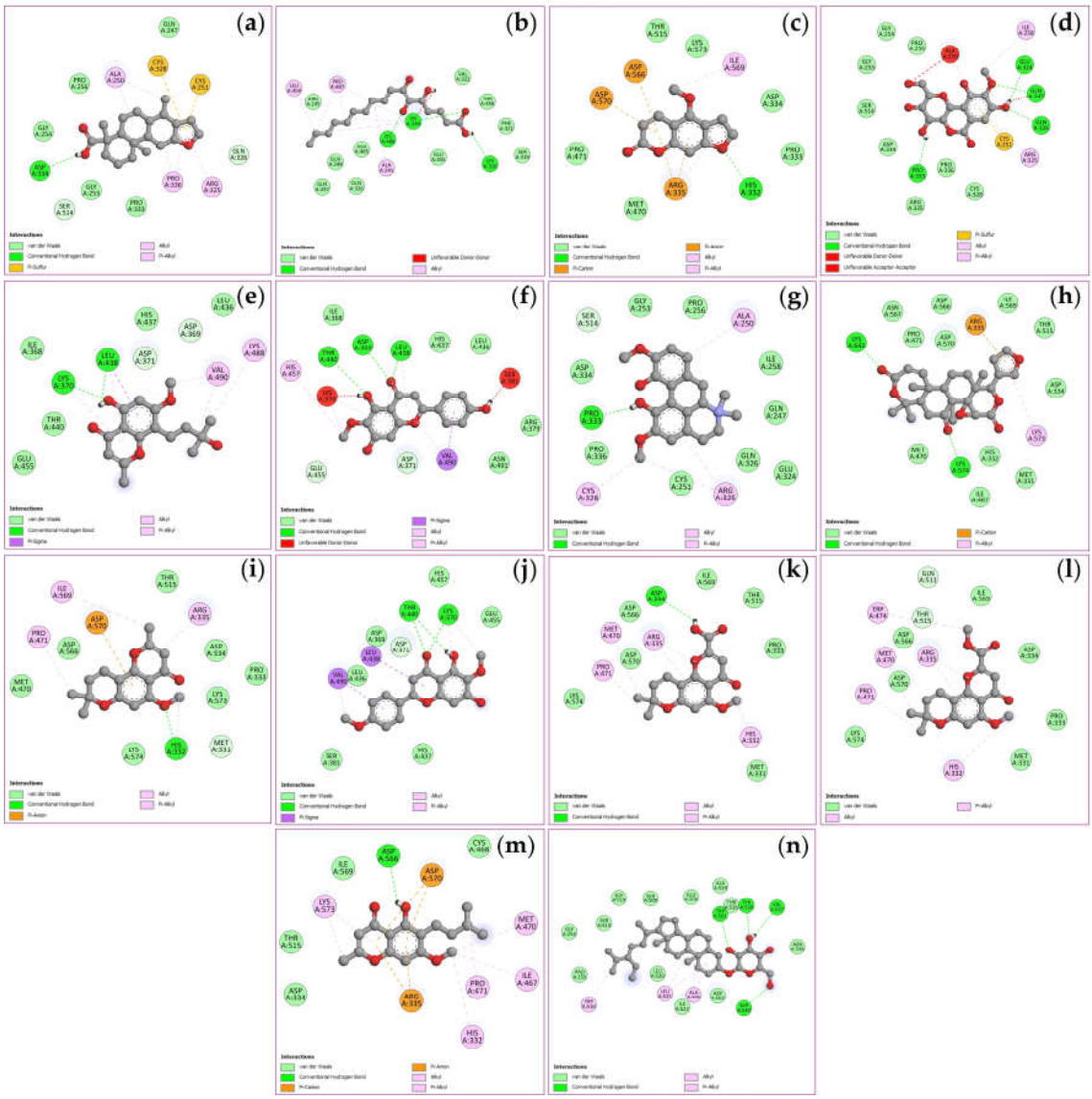

Figure 10. Visualization of molecular docking results for STAT3. The molecular docking models depict the interactions between bioactive compounds and STAT3: (+)-vouacapenic acid (**a**); 5, 7-dihydroxy-6-oxoheptadecanoic acid (**b**); bergapten (**c**); bergenin (**d**); harperamone (**e**); hispidulin (**f**); magnoflorine (**g**); obacunone (**h**); *O*-methylalloptaeroxylin (**i**); pectolinarigenin (**j**); perforatic acid (**k**); perforatic acid methyl ester (**l**); peucenin-7-methyl ether (**m**); stigmasterol glucoside (**n**).

 doi:10.20944/preprints202602.1199.v1

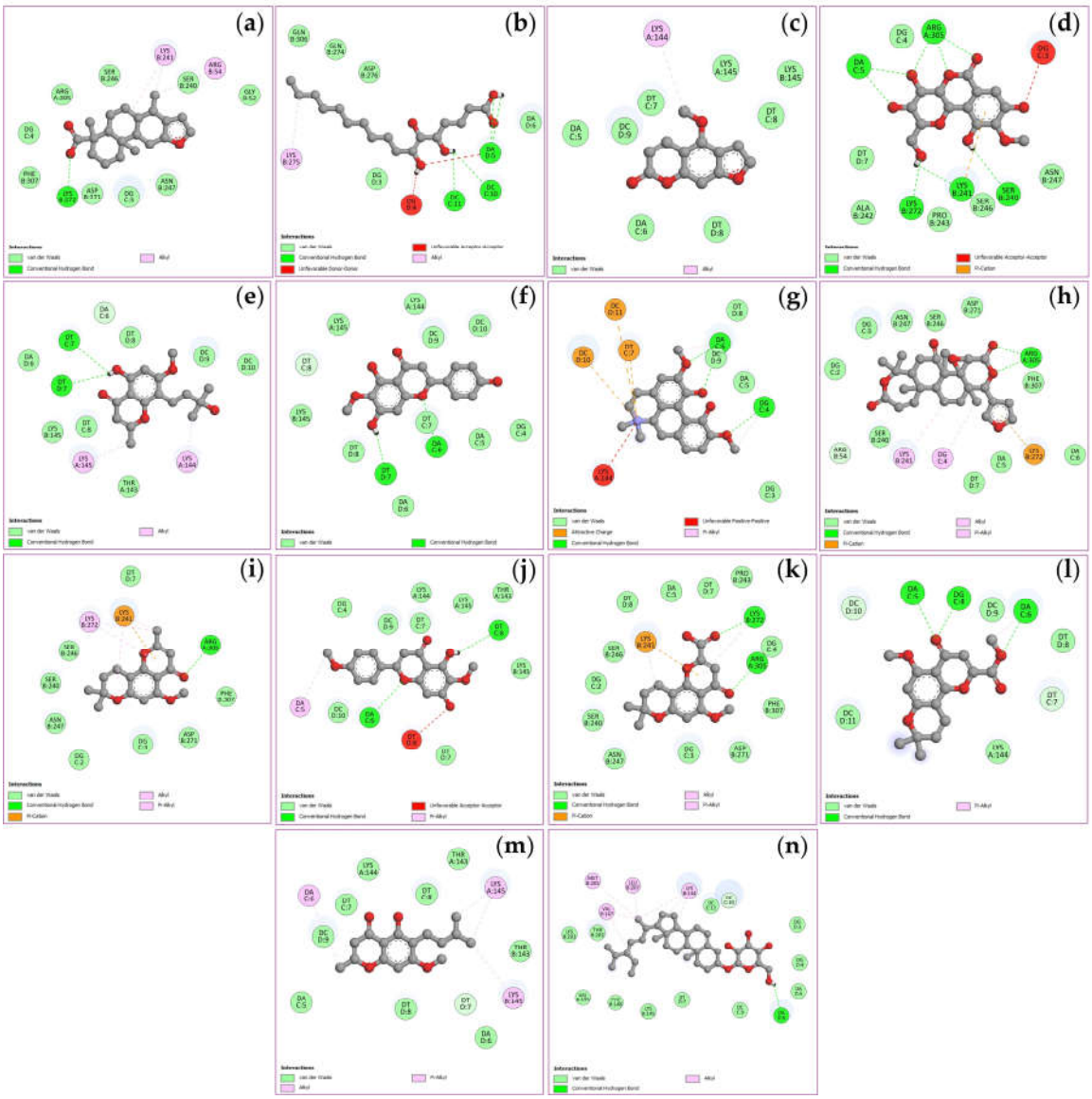

Figure 11. Visualization of molecular docking results for NFKB1. The molecular docking models depict the interactions between bioactive compounds and NFKB1: (+)-vouacapenic acid (**a**); 5, 7-dihydroxy-6-oxoheptadecanoic acid (**b**); bergapten (**c**); bergenin (**d**); harperamone (**e**); hispidulin (**f**); magnoflorine (**g**); obacunone (**h**); *O*-methylalloptaeroxylin (**i**); pectolinarigenin (**j**); perforatic acid (**k**); perforatic acid methyl ester (**l**); peucenin-7-methyl ether (**m**); stigmasterol glucoside (**n**).

2.7. Characterization of The BLW Extract

The HPLC chromatograms showing the major biomarker compounds are presented in Figure 12. The specific retention times for the five identified markers were determined as follows: bergenin (**1**) at 32.4 min, perforatic acid (**2**) at 92.9 min, *O*-methyllaloptaeroxyrin (**3**) at 104.6 min, pectolinarigenin (**4**) at 108.7 min, and peucenin-7-methyl ether (**5**) at 129.3 min. The chemical structures of these BLW biomarker compounds are depicted in Figure 13. Among these markers, perforatic acid (**2**), *O*-methylalloptaeroxylin (**3**), and peucenin-7-methyl ether (**5**) represent the primary constituents of *H. perforata*, while bergenin (**1**) and pectolinarigenin (**4**) are the major characteristic compounds of *F. racemosa* and *C. indicum*, respectively.

 doi:10.20944/preprints202602.1199.v1

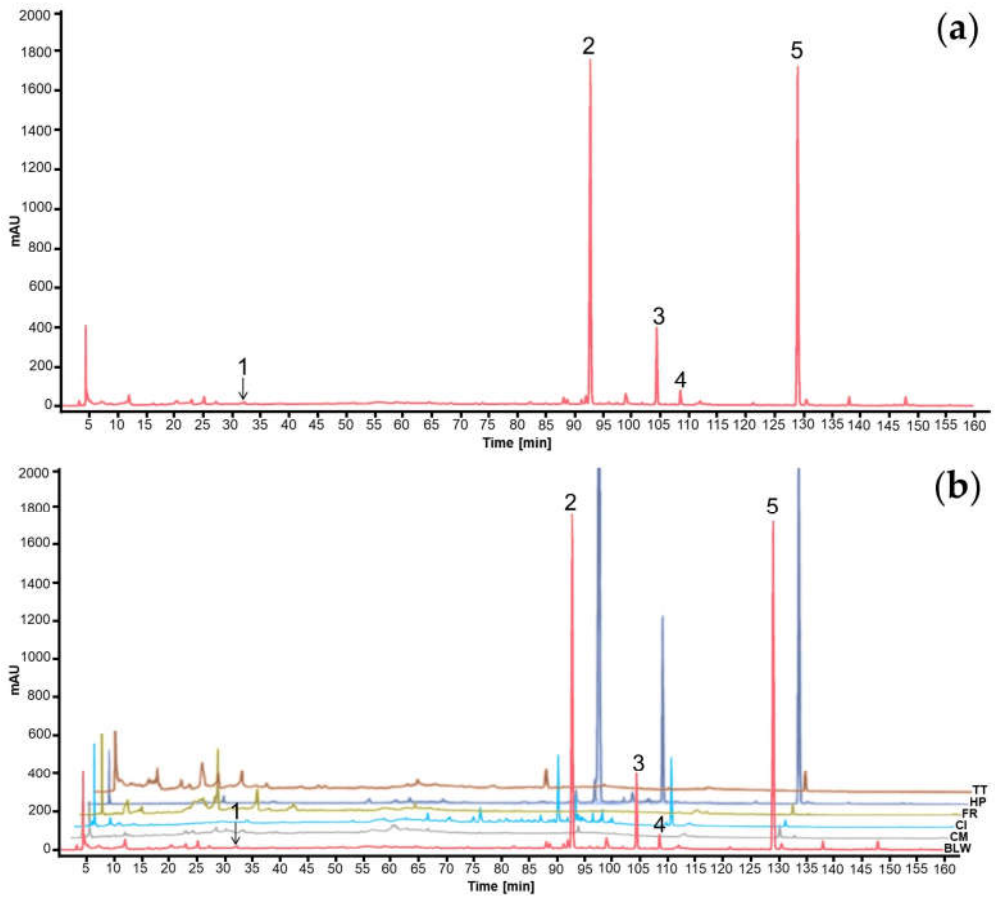

Figure 12. HPLC chromatogram of biomarker compounds for BLW extract (**a**) exhibiting the peaks of bergenin (**1**), perforatic acid (**2**), *O*-methyllaloptaeroxyrin (**3**), pectolinarigenin (**4**), and peucenin-7-methyl ether (**5**). HPLC chromatograms of Benjalokawichian (BLW) and its component plants (**b**), *Capparis micracantha* (CM), *Clerodendrum indicum* (CI), *Ficus racemosa* (FR), *Harrisonia perforata* (HP), *Tiliacora triandra* (TT).

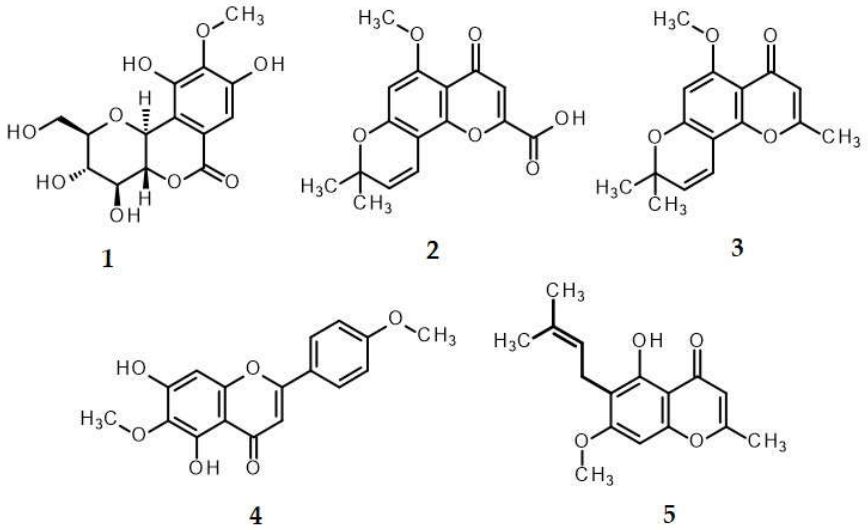

Figure 13. Chemical structures of the markers for the BLW extract: bergenin (**1**), perforatic acid (**2**), *O*-methyllaloptaeroxyrin (**3**), pectolinarigenin (**4**), peucenin-7-methyl ether (**5**).

The amount of the major compounds in the BLW extract was determined using a calibration curve of the reference standard. The linearity of the developed method was determined by R^2, which was assessed in six concentration levels as follows. Bergenin showed a linear equation of y = 31.112x

 doi:10.20944/preprints202602.1199.v1

+ 177.07 with the R^2 value of 1.0000. Perforatic acid showed y = 33.193x - 224.22 with the R^2 value of 0.9999. *O*-methylalloptaeroxylin showed y = 9.7555x + 173.69, with the R^2 value of 0.9996. Pectolinarigenin showed y = 41.603x - 5.8451 and the R^2 value of 1.0000. Peucenin-7-methyl ether showed y = 75.721x + 598.97 with the R^2 value of 0.9997. The BLW extract contained the highest amount of perforatic acid at 80.89 mg/g extract, followed by *O*-methylalloptaeroxylin and peucenin-7-methyl ether. On the contrary, pectolinarigenin, and bergenin were present in much lower amounts in the BLW extract (Table 4).

Table 4. The content of biomarkers in BLW and individual ingredient plant extracts.

Marker compounds	Content of biomarkers (mg/g extract)					
	BLW	CM	CI	FR	HP	TT
Bergenin (**1**)	0.22 ± 0.00^{a,*}	ND	ND	5.45 ± 0.01**	ND	ND
Perforatic acid (**2**)	80.89 ± 0.00^{b,*}	ND	ND	ND	288.39 ± 0.00^{a,**}	ND
O-Methyllaloptaeroxyrin (**3**)	53.29 ± 0.02^{c,*}	ND	ND	ND	216.46 ± 0.03^{b,**}	ND
Pectolinarigenin (**4**)	2.50 ± 0.00^{d,*}	ND	3.76 ± 0.00*	ND	ND	ND
Peucenin-7-methyl ether (**5**)	35.03 ± 0.00^{e}	ND	ND	ND	73.51 ± 0.00^{c,**}	ND

Values are expressed as mean ± SD of triplicate measurements (n = 3). Different superscript letters ($^{a, b, c, d, e}$) in the same column and different symbols (*,**) in the same row indicate significant differences between groups ($p < 0.01$). Benjalokawichian (BLW); *Capparis micracantha* (CM); *Clerodendrum indicum* (CI); *Ficus racemosa* (FR); *Harrisonia perforata* (HP); *Tiliacora triandra* (TT); not detected (ND).

2.8. Effects of the BLW Extract and Biomarker Compounds on NO Production in LPS-Induced RAW264.7 Macrophages

The BLW extract effectively suppressed nitric oxide (NO) production in LPS-stimulated RAW 264.7 macrophages, yielding an IC_{50} value of 69.10 μg/mL. Notably, at a concentration of 100 μg/mL, the BLW extract demonstrated superior potency compared to the positive control, indomethacin, which had an IC_{50} of 73.42 μg/mL. The inhibitory activity of the BLW extract was dose-dependent within the concentration range of 50 to 100 μg/mL. Among the individual components of BLW, the extract of *T. triandra* exhibited the most significant inhibitory effect, with an IC_{50} of 45.71 μg/mL, followed by the extract of *F. racemosa*, with an IC_{50} of 65.71 μg/mL. Conversely, the remaining single-herb extracts showed limited activity, with IC_{50} values exceeding 100 μg/mL. It is worth noting that the *H. perforata* extract displayed a dose-dependent response in the concentration range of 10 to 100 μg/mL. Interestingly, all tested marker compounds were significantly less effective than indomethacin when evaluated at 100 μg/mL. However, specific compounds showed characteristic dose-dependent trends as shown in Figure 14. Perforatic acid exhibited dose-dependent inhibition at concentrations of 1 to 100 μg/mL, while peucenin-7-methyl ether exhibited a similar behavior at concentrations of 10 to 100 μg/mL.

 doi:10.20944/preprints202602.1199.v1

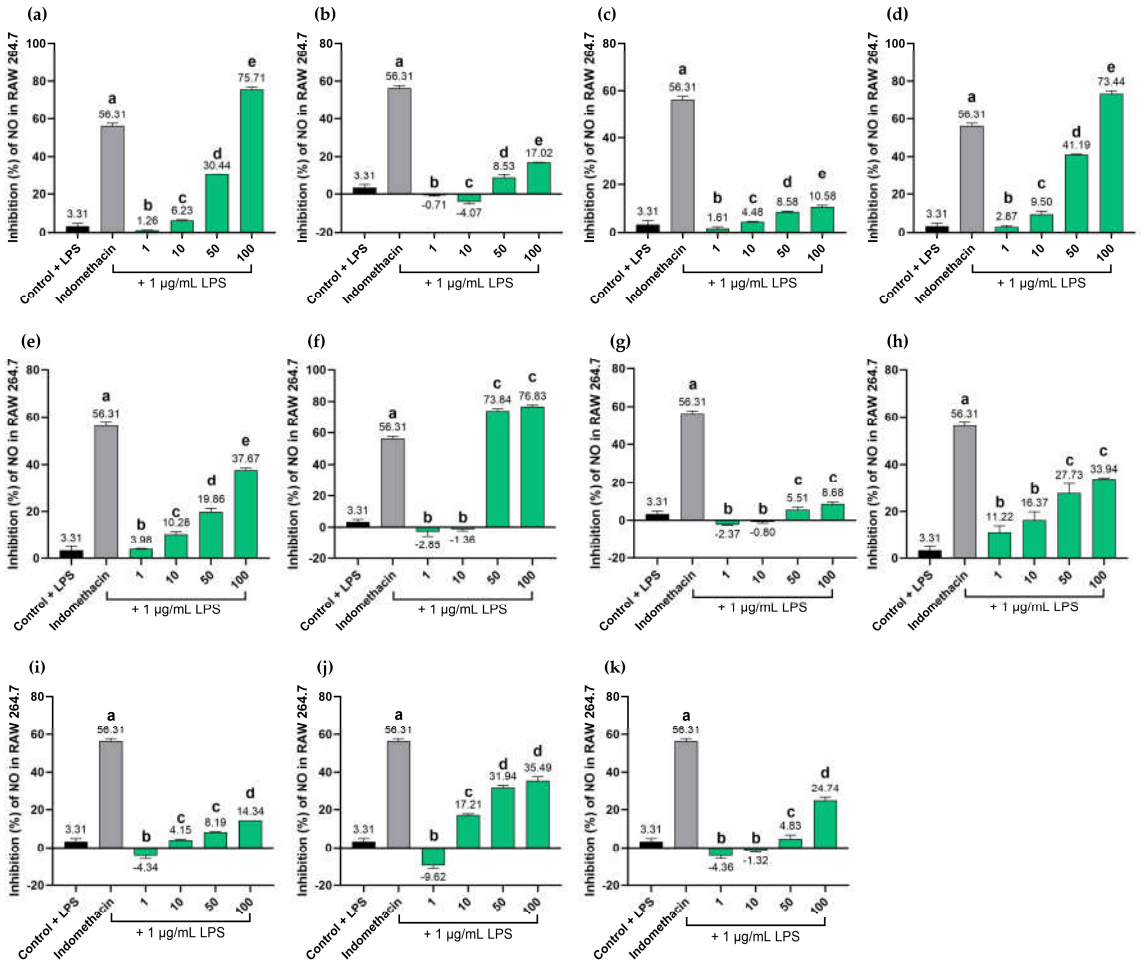

Figure 14. Inhibition of nitric oxide (NO) production by BLW extract and marker compounds at concentrations of 1-100 μg/mL on LPS-induced RAW264.7 macrophages: BLW extract (**a**); *C. micracantha* extract (**b**); *C. indicum* extract (**c**); *F. racemosa* extract (**d**); *H. perforata* extract (**e**); *T. triandra* extract (**f**); bergenin (**g**); perforatic acid (**h**); *O*-methyllaloptaeroxyrin (**i**); pectolinarigenin (**j**); peucenin-7-methyl ether (**k**). Bars with different letters indicate significant differences ($p < 0.01$). Values are expressed as mean ± SD (n = 3). Indomethacin at 100 μg/mL was used as a positive control.

2.9. Cytotoxicity Effects of the BLW Extract and Biomarker Compounds on RAW264.7 Macrophages

The cytotoxicity of the BLW extract and the extracts of its individual components was evaluated using RAW 264.7 macrophages. Results indicated that the BLW extract, along with extracts of *C. micracantha*, *C. indicum*, *F. racemosa*, and *H. perforata*, as well as the biomarkers, bergenin, perforatic acid, and *O*-methylalloptaeroxylin, did not affect cell viability within the concentration range of 1 to 100 μg/mL. However, at the maximum tested concentration of 100 μg/mL, several treatments, *viz.*, the BLW extract, bergenin, perforatic acid, pectolinarigenin, and peucenin-7-methyl ether, resulted in significantly lower cell viability compared to indomethacin (a positive control), except for *O*-methylalloptaeroxylin, which maintained a percentage of cell viability comparable to that of indomethacin. Notably, the extract of *T. triandra* exhibited cytotoxic effects when administered at 100 μg/mL. Furthermore, the cytotoxicity of pectolinarigenin exhibited a clear dose-dependent trend, where cell viability decreased as the concentration increased, as shown in Figure 15.

 doi:10.20944/preprints202602.1199.v1

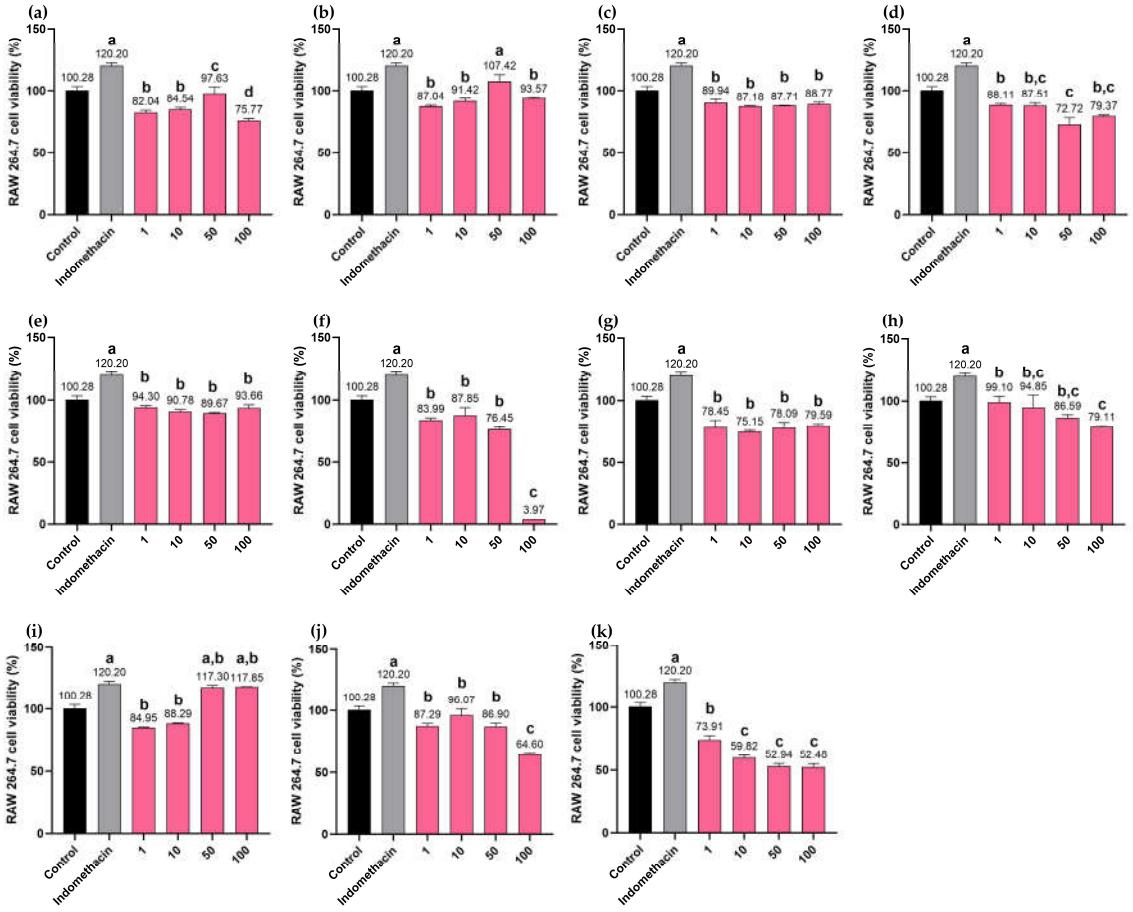

Figure 15. Cell viability of macrophage RAW264.7 treated with BLW extract and marker compounds at concentrations 1-100 μg/mL: BLW extract (**a**); *C. micracantha* extract (**b**); *C. indicum* extract (**c**); *F. racemosa* extract (**d**); *H. perforata* extract (**e**); *T. triandra* extract (**f**); bergenin (**g**); perforatic acid (**h**); *O*-methyllaloptaeroxyrin (**i**); pectolinarigenin (**j**); peucenin-7-methyl ether (**k**). Bars with different letters indicate significant differences ($p < 0.01$). Values are expressed as mean ± SD (n = 3). Indomethacin at 100 μg/mL was used as a positive control.

3. Discussion

Toxic fever (TF) is characterized by a sudden and severe high fever, which is frequently associated with serious infections and inflammatory processes [10]. In Thai traditional medicine, a polyherbal remedy known as BLW has been used to alleviate TF. This remedy is also reported to modulate inflammatory conditions [11,12]. Polyherbal remedies are gaining popularity in both modern and traditional medicine. The underlying logic of these botanical formulations is centered on the interaction of diverse bioactive constituents. This multicomponent strategy is designed to improve therapeutic efficacy by employing a holistic approach to health and wellness. The synergistic interaction among the constituents of different herbs can complement and potentiate individual therapeutic effects, minimize adverse reactions, and improve overall treatment efficacy. Polyherbal remedies provide multi-targeted treatment, addressing the root causes like oxidative stress or immune system dysregulation [6,20,21]. However, despite their advantages, many aspects, such as the mechanism of action, identification of active compounds, standardization, quality control, and regulatory approval, are still serious obstacles for polyherbal remedies to be accepted in mainstream medicine [20]. Network pharmacology can serve to provide a possible interpretation of the complex relationships among active ingredients, targets, and diseases, which can elucidate the multi-target mechanism in many traditional medicines, especially in the Traditional Chinese Medicine (TCM), to reveal the possible therapeutic pathways from a holistic and comprehensive perspective [22].

 doi:10.20944/preprints202602.1199.v1

This research applied an integrated approach, combining network pharmacology and molecular docking to investigate the potential mechanisms by which the BLW remedy exerts its effects in the treatment of TF. Through a systematic process of screening bioactive constituents, identifying therapeutic protein targets, and evaluating protein–protein interaction networks, our study allowed us to map the complex interplay between the remedy and the disease.

Widely reported metabolic changes during fever, metabolomics, and network pharmacology analyses have revealed distinct biomarkers and gene targets under varying conditions [14–16]. Literature review suggests that BLW comprises 17 bioactive constituents with 495 genes. This study identified 8,031 TF-associated genes, 88 of which overlapped with BLW targets. These common genes regulate vital processes such as inflammation, apoptosis, and cell differentiation. Notably, TNF, PTGS2, STAT3, and NFKB1 were identified as the highest-connectivity targets within the network. Their strong binding affinities with the 17 BLW compounds were further validated through molecular docking, confirming their central role in the therapeutic mechanism.

Network pharmacology and molecular docking are established methods for identifying bioactive constituents and their corresponding targets in studies of fever. A prominent example includes the analysis of Xiaochaihu Decoction, where 726 bioactive compounds were retrieved from the traditional Chinese medicine systems pharmacology (TCMSP) database. This remedy was associated with 677 targets. Furthermore, research identified 7,305 fever-related genes, with 400 key targets directly relevant to the treatment of febrile conditions. Previous research underscores the efficacy of network pharmacology in identifying bioactive compounds for febrile conditions. For instance, GAPDH, AKT1, INS, IL6, and VEGFA were established as primary targets in related studies [14]. Similarly, analysis of Bai Hu Tang was able to identify 120 active compounds and 2,176 targets, leading to the selection of 34 therapeutic candidates, including TNF, CASP1, PTGS2, and IL6R [15]. Furthermore, Zi Xue Powder was found to contain 126 active compounds linked to 707 potential targets, with ALB, AKT1, INS, TNF, and IL6 emerging as pivotal proteins [16]. Despite differences in herbal composition and specific chemical constituents, these remedies share common biological mechanisms. Previous studies consistently highlighted the regulation of cell proliferation, apoptosis, and inflammation as central to the antipyretic effect [14–16]. Notably, while the current study identified a more focused set of active compounds, it successfully mapped a significantly larger number of target genes than previous reports. Most importantly, this research reveals that the therapeutic potential of BLW is highly enriched in the phenylalanine and arachidonic acid metabolism pathways, both of which play critical roles in modulating fever and inflammatory responses.

The 88 identified therapeutic targets form a complex and interconnected network where nodes and edges represent individual proteins and their interactions. Within this system, higher node degrees indicate more significant functional roles. Notably, four core proteins consisting of TNF, PTGS2, STAT3, and NFKB1 serve as central hubs. These proteins play synergistic roles in regulating infection, inflammation, cell proliferation, and apoptosis in TF. Their clustering into the primary functional module underscores their importance as pivotal therapeutic targets for the BLW remedy. Current evidence suggests that fever onset is primarily triggered by cytokines such as TNF, IL6, and IL1B. These mediators activate phospholipase A2 (PLA_2) to convert phospholipids into arachidonic acid, which is subsequently metabolized to PGH_2 by COX-2. Increased expression of COX-2 and mPGES-1 leads to the generation of PGE_2 within the central nervous system. As a principal mediator of fever, PGE_2 binds to EP3 receptors on hypothalamic neurons, signaling the brain to elevate the body's thermal set point [1,2,4,5]. TNF contributes to fever induction through mechanisms dependent on IL6 plasma levels but independent of IL1B. While exogenous TNF-induced fever involves peripheral IL1 release, intravenous injection of recombinant human TNF (rhTNF) triggers pyrogenicity through glutathione-associated PGE_2 production. Furthermore, IL6 interacts with receptors on brain endothelial cells to induce COX-2 expression via the STAT3 signaling pathway. Simultaneously, IL1 activates the NF-κB (nuclear factor kappa-light-chain-enhancer of activated B

 doi:10.20944/preprints202602.1199.v1

cells) pathway to promote COX-2 production in cerebral endothelial cells, thereby facilitating PGE_2 synthesis [23].

On the basis of ADME (absorption, distribution, metabolism, and excretion) criteria with parameters set for high gastrointestinal absorption and a drug-likeness (DL) of 1, several plant constituents in BLW are considered highly promising. Specifically, 5,7-dihydroxy-6-oxoheptadecanoic acid, harperamone, hispidulin, magnoflorine, obacunone, *O*-methylalloptaeroxylin, pectolinarigenin, perforatic acid, and perforatic acid methyl ester were found to interact with ten or more targets. These findings suggest that these compounds may contribute significantly to the pharmacological activity of BLW in treating TF. It is essential to note that the therapeutic efficacy of BLW stems from the synergistic action of its complex chemical composition rather than isolated constituents. Recent analysis identified perforatic acid and *O*-methylalloptaeroxylin as major components, while pectolinarigenin was classified as a minor constituent. Despite its lower concentration, *O*-methylalloptaeroxylin exhibited potent anti-inflammatory activity by significantly inhibiting NO production in LPS-induced RAW 264.7 macrophages, with an IC_{50} of 7.92 μg/mL [24]. Furthermore, pectolinarigenin has been shown to modulate the inflammatory response by inhibiting LPS-induced NF-κB activation through the stabilization of IκB-α (nuclear factor of kappa light polypeptide gene enhancer in B-cells inhibitor alpha). This compound regulates the NF-κB/Nrf2 signaling pathways, subsequently suppressing the synthesis of pro-inflammatory mediators, *viz*., iNOS, COX-2, IL6, IL1B, and TNF [25]. Previous studies on pectolinarigenin, isolated from BLW, further support these findings, reporting strong inhibition of NO production with an IC_{50} of 7.15 μg/mL [24].

GO enrichment analysis was performed to elucidate the functional roles of potential therapeutic targets and their mechanisms in overcoming TF resistance. The BP associated with BLW targets were primarily linked to cardiac function, apoptosis regulation, cell proliferation, and the inflammatory response. These findings are particularly relevant to TF, which is characterized by high fever often resulting from severe infection and systemic inflammation [10]. Key targets identified in this study, including cytokines like TNF and inflammatory enzymes such as PTGS2, play critical roles in modulating the inflammatory microenvironment of TF [1,2,4,5]. Regarding MF, the targets exhibited specific activities such as prostaglandin-endoperoxide synthase, aliphatic-amine oxidase, and G-protein coupled adenosine receptor activity. These functions also encompassed broader categories, viz., protein, enzyme, and energy substance binding. Furthermore, CC analysis localized these activities to specific substructures like the endolysosome lumen, nuclear envelope lumen, and histone deacetylase complex. These intracellular sites are intrinsically associated with inflammatory pathways, cellular turnover, pyretic responses, and RNA transcription. Such localization supports the therapeutic potential of BLW in managing TF by modulating specific proteins involved in its pathophysiology, notably TNF, PTGS2, STAT3, and NFKB1 [1]. These results reinforce the multi-dimensional approach of the BLW remedy in targeting the molecular foundations of fever and inflammation.

KEGG enrichment analysis identified several signaling pathways critical to the anti-TF mechanism of BLW. Core gene targets were significantly enriched in phenylalanine, tyrosine, and arachidonic acid metabolism pathways. Modulating these pathways directly influences biological processes associated with infection, inflammation, and cellular turnover, suggesting that BLW may also play a role in mitigating chemotherapy resistance. The phenylalanine and tyrosine metabolism pathways are well-recognized for their involvement in inflammatory diseases and severe fever [26]. Specifically, inflammatory states frequently lead to a marked increase in the serum phenylalanine-to-tyrosine ratio, a phenomenon observed in various infectious diseases, *viz*., viral encephalitis and yellow fever [27]. Furthermore, the arachidonic acid metabolism pathway is central to fever induction. Pro-inflammatory cytokines such as TNF, IL6, and IL1B initiate the release of arachidonic acid from membrane phospholipids, which was subsequently converted to PGH_2 by COX-2. The final step involving mPGES-1 activity results in the production of PGE_2, the primary mediator of the febrile response [1–6]. The therapeutic potential of BLW through these metabolic routes is supported by

 doi:10.20944/preprints202602.1199.v1

multiple studies. The ethanolic extract of BLW has been shown to suppress COX-2 expression and reduce PGE_2 levels in IL1B-stimulated human umbilical vein endothelial cells [3]. Additionally, BLW effectively decreased TNF and IL1B levels in LPS-induced macrophages, with IC_{50} values of 103.96 and 60.09 μg/mL for TNF and PGE_2 inhibition, respectively [28]. In vivo evidence further validated these findings. Oral administration of BLW powder at doses ranging from 300 to 3,000 mg/kg reduced plasma TNF and IL1B in rats with systemic inflammation [29]. Regarding antipyretic efficacy, BLW powder was effective against yeast-induced fever [30]. Moreover, oral administration of BLW extract at doses of 300 mg/kg or within a range of 25 to 400 mg/kg exhibited potency comparable to acetylsalicylic acid in reducing rectum temperature in LPS-induced fever models [31].

Molecular docking revealed the interaction between compounds and targets in the network pharmacology. Results indicated that obacunone exhibited the strongest binding affinity with the TNF, STAT3, and NFKB1 receptors, which is consistent with the finding of Luo et al., who reported the suppression of the protein levels of pro-inflammatory cytokines (TNF, iNOS, COX-2) and phosphorylation of the NF-κB complex by obacunone [32]. Moreover, obacunone, isolated from the roots of *H. perforata*, was found to inhibit LPS-induced NO production in RAW 264.7 macrophages, with an IC_{50} of 83.61 μM [33], while hispidulin, a constituent of *C. indicum*, exhibited the strongest binding affinity with the PTGS2 receptor [34]. Yu et al. reported a significant reduction of the levels of NO, ROS, iNOS, COX-2, TNF, IL1B, IL6, and PGE_2 by hispidulin, in a dose-dependent manner, suggesting this compound may inhibit neuroinflammatory responses through NF-κB pathway inhibition [35]. Additionally, marker compounds in BLW, i. e. bergenin, perforatic acid, *O*-methyllaloptaeroxyrin, pectolinarigenin, and peucenin-7-methyl ether show strong binding to protein.

In this work, the biomarkers used for HPLC analysis of the BLW extract are bergenin, perforatic acid, *O*-methyllaloptaeroxyrin, pectolinarigenin, and peucenin-7-methyl ether. Bergenin, an isocoumarin glycoside, is a constituent of *F. racemosa* root [36,37], while the chromones perforatic acid, *O*-methyllaloptaeroxyrin, and peucenin-7-methyl ether are constituents of *H. perforata* root [38,39], and the isoflavone pectolinarigenin is a constituent of *C. indicum* root [40,41]. It is worth mentioning that all the biomarkers used to characterize the BLW extract in this study possess anti-inflammatory activity [24,33,42–44]. The HPLC chromatogram showed that perforatic acid, *O*-methyllaloptaeroxyrin, and peucenin-7-methyl ether are major peaks, while bergenin and pectolinarigenin constitute minor comounds. It is worth mentioning that some authors have used different markers such as pectolinarigenin [40,41], tiliacorinine, yanangcorinine [45], and lupeol [46,47] for HPLC fingerprint analysis of this polyherbal remedy.

Inflammation is one of the mechanisms of fever. In fever reactions, pro-inflammatory cytokines such as COX-2, TNF, IL1B, IL6, and NF-κB trigger the expression of the inducible nitric oxide synthase (iNOS) in monocytes or macrophages, neutrophil granulocytes, and many other cells. However, in the case of bacterial infection, endotoxin is another strong inducer of iNOS expression. Consequently, large amounts of NO are synthesized, exceeding the physiological NO production by up to 1000-fold [48–51]. In this study, the BLW extract potently inhibited NO production in LPS-induced RAW264.7 macrophages, with an IC_{50} value of 69.10 μg/mL. This finding was in agreement with the studies by Juckmeta and Itharat (2012), who reported the IC_{50} values of 40.36 μg/mL [52], and by Kaewnoi et al. (2024), who reported the IC_{50} of 97.38 μg/mL for ethanol extracts of BLW in the same model [28]. *T. triandra* and *F. racemosa* were the only single-herb extracts to exhibit potent inhibition of NO production, with IC_{50} values of 45.71 and 65.71 μg/mL, respectively, while the remaining single-herb extracts showed only weak inhibitory activity. Our findings are also in agreement with the previous report by Juckmeta and Itharat, which used the ethanolic extracts of the same plants and the same assay model. They obtained the IC_{50} values for NO inhibition of 61.35 μg/mL for *C. micracantha*, 46.55 μg/mL for *C. indicum*, 53.16 μg/mL for *H. perforata*, and 54.65 μg/mL for *T. triandra*. Furthermore, they have also found that *F. racemosa* showed only weak inhibitory activity [52]. In this study, the individual biomarkers bergenin, perforatic acid, *O*-methyllaloptaeroxyrin, pectolinarigenin, and peucenin-7-methyl ether generally showed weak NO

 doi:10.20944/preprints202602.1199.v1

inhibitory activity (IC_{50} > 100 μg/mL). However, perforatic acid exhibited a dose-dependent inhibition of NO production at the concentration range of 1-100 μg/mL, while peucenin-7-methyl ether showed dose-dependent NO inhibition in the concentration range of 10-100 μg/mL.

There are several reports of the anti-inflammatory activity of bergenin, *O*-methylalloptaeroxylin, pectolinarigenin, and peucenin-7-methyl ether. Gao et al., in their study of the effects and mechanism of bergenin on the mammary glands during LPS-induced mastitis in a mouse model, have found that bergenin reduced the expression of NO, TNF, IL1B, and IL6 proinflammatory cytokines by inhibiting the activation of the NF-κB and MAPKs signaling pathways [42]. Intriguingly, although perforatic acid, *O*-methyllaloptaeroxyrin, and peucenin-7-methyl ether are major compounds that exhibited strong binding to proteins, they showed weak NO inhibitory activity. On the contrary, Juckmeta has found the inhibition of NO production in LPS-induced RAW264.7 macrophages by *O*-methylalloptaeroxylin and pectolinarigenin, with IC_{50} values of 7.92 and 7.15 μg/mL, respectively [24], while Choodej et al. reported the NO inhibition by peucen-in-7-methyl ether, with an IC_{50} of 56.36 μM [33].

The extracts of BLW, *C. micracantha*, *C. indicum*, *H. perforata*, *F. racemosa* and the biomarkers, *viz.* bergenin, perforatic acid, and *O*-methylalloptaeroxylin showed no cytotoxicity against RAW264.7 macrophages at concentrations where cell viability remained above 70%. However, pectolinarigenin and peucenin-7-methyl ether exhibited increased cytotoxicity at higher concentrations. Only the *T. triandra* extract displayed cytotoxicity at the highest tested concentration (100 μg/mL), however, the extract showed no cytotoxicity at a concentration of 50 μg/mL. These findings are consistent with previous reports of non-toxicity of the BLW extract in macrophage cell lines [28,52], in rats [29], and in humans [53].

Although results obtained from integrated network pharmacology indicated the TNF, COX-2, STAT3, and NFKB1 signaling pathways may play important roles in fever relief, they are still predictive and require further experimental validation. Moreover, while the BLW extract showed a dose-dependent reduction of NO production in LPS-induced RAW264.7 macrophages, this in vitro model represents only a simplified aspect of the TF microenvironment. Pro-inflammatory cytokines such as TNF, IL6, and IL1B are known to stimulate the gene expression of iNOS, which generates large amounts of NO [48–51]. Consequently, the ability of the BLW extract and its phytochemicals to inhibit NO production serves as a direct indicator of their anti-inflammatory activity. As a life-sustaining process, it is highly complex, and dysregulation has been linked to diverse pathological conditions, including fever. Therefore, additional in vivo and clinical studies will be required to validate these mechanistic insights.

4. Materials and Methods

4.1. Screening for Potential Bioactive Compounds and BLW-Related Targets

To identify potential bioactive compounds in the BLW remedy, an extensive literature review was conducted using several electronic platforms, including PubMed/Medline, ScienceDirect, ISI Web of Science, and ClinicalTrials.gov. Moreover, the search for compounds from the five medicinal plants in BLW with reported anti-inflammatory or antipyretic properties from Thai research databases was also carried out. The identified bioactive compounds were then screened using the SwissADME database (http://www.swissadme.ch/, accessed on 24 November 2023) [54], based on two key ADME indices, i. e. GI absorption, which evaluates a compound's property to be absorbed in the GI after an oral administration, and drug-likeness, which assesses the likelihood of a molecule to become an orally bioavailable drug. The cut-off criteria were set as follows: GI absorption = High and Drug likeness = 1. Next, the selected compounds were retrieved from the PubChem database (https://pubchem.ncbi.nlm.nih.gov/, accessed on 24 November 2023) [55] to obtain their chemical structures using the Simplified Molecular Input Line Entry System (SMILES). Potential therapeutic targets of BLW were then predicted using the SwissTargetPrediction database

 doi:10.20944/preprints202602.1199.v1

(http://www.swisstargetprediction.ch/, accessed on 24 November 2023) [56] with targets having a probability of greater than 0 selected for further analysis.

4.2. Identification of TF-Related Targets

Three databases were used to identify potential targets related to TF. The GeneCards database (https://www.genecards.org/, accessed on 10 January 2024) [57] provides comprehensive information on all annotated and predicted human genes, integrating data from 150 web sources, including genomic, transcriptomic, proteomic, genetic, clinical, and functional information. The OMIM database (https://omim.org/, accessed on 11 January 2024) [58] serves as a detailed repository of human genes and genetic phenotypes, covering over 16,000 genes and all known Mendelian disorders, with daily updates. Additionally, the PharmGKB database (https://www.pharmgkb.org/, accessed on 12 January 2024) [59] was used to gather pharmacogenomic information on genes associated with TF. Targets identified from these databases were merged and categorized as TF-related targets for further analysis.

4.3. Protein-Protein Network Interaction and Modular Identification

The STRING database (https://string-db.org, accessed on 18 February 2024) is widely used in bioinformatics to predict and construct protein-protein interaction (PPI) networks [60]. The STRING platform was used to examine the intersection between targets related to BLW and TF for assessing their potential as therapeutic candidates. By processing relevant gene sets, interaction data were extracted to establish a PPI network. This network was specifically curated for Homo sapiens and utilized a medium confidence threshold of 0.4 to maintain the validity of the interactions. To evaluate the network's architecture, Cytoscape (v3.10.2) was used to compute key topological parameters, including the degree value, closeness centrality, and betweenness centrality. Furthermore, the MCODE plugin was applied to identify highly connected clusters or central nodes within the network, using a configured degree cut-off of 2, a k-core of 2, a node score cut-off of 1.0, and a maximum depth of 100.

4.4. Functional Enrichment and Pathway Analysis

DAVID Bioinformatics Resources 6.8 (https://davidbioinformatics.nih.gov/, accessed on 15 March 2024) [61], was used to analyze all potential therapeutic targets through GO and KEGG pathway enrichment. The objective of this analysis was to determine relevant biological pathways and GO terms, categorized into BP, MF, and CC. Only pathways and GO terms exhibiting a p-value of less than 0.05 were considered statistically significant and selected for subsequent evaluation. To represent the findings of the GO and KEGG enrichment analyses, bubble plots illustrating signaling pathways and GO classifications were generated via the Bioinformatics online platform (http://www.bioinformatics.com.cn/, accessed on April 21, 2023). Furthermore, the complex interactions between bioactive substances, candidate targets, and associated signaling pathways were mapped and visualized using Cytoscape (version 3.10.2).

4.5. Verification with Molecular Docking

4.5.1. Protein Structures and Modeling of Ligands Preparation

The three-dimensional (3D) crystal structures of four potential human therapeutic targets were retrieved from the Brookhaven Protein Data Bank (http://www.rcsb.org/, accessed on May 19, 2024). These targets included TNF (tumor necrosis factor-α, PDB ID: 2AZ5), PTGS2 (prostaglandin-endoperoxide synthase 2, PDB ID: 3LN1), STAT3 (signal transducer and activator of transcription 3, PDB ID: 6NJS), and NFKB1 (nuclear factor kappa subunit 1, PDB ID: 1NFK). All selected protein models possessed a resolution of 2.5 Å. During the acquisition process, the complete structural data of the proteins were obtained, along with information regarding their respective small-molecule ligands. For molecular docking, TNF utilized chain protein D [62], while PTGS2 used chain protein

 doi:10.20944/preprints202602.1199.v1

A [63]. The STAT3 unit contains two domains: a DNA-binding domain and a SH2 domain [64]. NFKB1 was removed from the structure p50 dimer and p50 monomers (chains A and B) [65]. The three-dimensional coordinates of the 15 bioactive compounds were retrieved from the PubChem database (https://pubchem.ncbi.nlm.nih.gov/, accessed on May 19, 2024). In the preparation phase, Discovery Studio 2021 was utilized to remove water molecules and pre-existing ligands from the protein structures, which were then exported as PDB files. Subsequently, AutoDockTools (version 1.5.6) was used to facilitate the addition of hydrogen atoms, charge calculation, and the merging of nonpolar hydrogens. To finalize the docking inputs, both the target receptors and small-molecule ligands were converted into PDBQT formats. Within these files, all active bonds in the ligands were configured as rotatable to account for molecular flexibility during the simulation.

4.5.2. Protein-Ligand Docking

Molecular docking was performed using AutoDock Vina 4 [66], chosen for its high processing speed and superior ability to predict binding models. To validate the docking protocol, the spatial conformations of the docked ligands were compared against their original crystal-bound positions. The molecular docking simulations were performed using a setting of 100 binding modes (num_modes). Furthermore, the dimensions of the grid box and its coordinates were established based on parameters identified from prior literature reviews to ensure optimal binding site coverage. The docking site for TNF was defined within a cube of 40 × 40 × 40 Å, covering the ligand-binding site, with a grid point spacing of 1.0 Å, centered at x = -11.9784, y = 70.2727, and z = 14.7429) [62]. For PTGS2 was set within a cube of 30 × 30 × 30 Å, with a grid point spacing of 1.0 Å, centered at x = 31.724, y = -22.006, and z = -17.132 [63]. The docking site for STAT3 was defined using a cube of 72 × 74 × 48 Å, with a grid point spacing of 2.7 Å, centered at x = 7.202330, y = 31.187204, and z = 20.437019 [64]. Finally, the docking site for NFKB1 was set within a cube of 30 × 30 × 30 Å, with a grid point spacing of 0.3 Å, centered at x = -1.1958, y = 9.0149, and z = 19.7598 [65].

4.5.3. Docking Validation

Molecular docking simulations were performed to assess the binding affinities between the identified bioactive constituents and their respective protein targets. These targets were selected based on the overlap between the four primary hub proteins and those with the most extensive interaction profiles. In terms of thermodynamic evaluation, a binding energy of less than 0 kJ/mol corresponds to spontaneous ligand-receptor association, whereas a value lower than -4.0 kJ/mol reflects a robust binding affinity. The docking methodology was validated by retrieving the 3D structures of known inhibitors for these four human therapeutic targets from PubChem and academic literature. This validation process was performed using AutoDockTools 1.5.6, adhering to the identical experimental parameters used for the bioactive compounds. The validation ligands included thalidomide (CID: 5426) as an inhibitor of TNF [67], celecoxib (CID: 2662) as an inhibitor of PTGS2 [68], ochromycinone (CID: 11808929) as an inhibitor of signal transducer and activator of transcription 3 (STAT3) [69] and selinexor (CID: 71481097) as an inhibitor of nuclear factor-κB (NFKB1) [70].

4.6. Preparation of BLW Extract

The roots of five plants, namely *Capparis micracantha* DC. (MSU.PH-CAP-C1), *Clerodendrum indicum* (L.) Kuntze (MSU.PH-LAM-C1), *Ficus racemosa* L. (MSU.PH-MOR-F1), *Harrisonia perforata* (Blanco) Merr. (MSU.PH-RUT-H1), and *Tiliacora triandra* Diels (MSU.PH-MEN-T1), were harvested from Roi Et Province in Northeast Thailand in October 2022. Taxonomical identification was performed by Assoc. Prof. Dr. Somsak Nualkaew, and the voucher specimens were deposited at the Pharmaceutical Chemistry and Natural Products Research Unit, Faculty of Pharmacy, Mahasarakham University, Thailand. Regarding the extraction process, the fresh roots were thoroughly washed, sliced in small pieces, and subjected to dehydration in a hot-air oven at 45 °C for

 doi:10.20944/preprints202602.1199.v1

72 hours. The dried plant materials were subsequently reduced into coarse powders. To prepare the BLW remedy, equal amount of powdered samples were mixed thoroughly together and macerated in 70% ethanol at a 1:5 (w/v) ratio for three days with periodic agitation. The mixture was filtered through Whatman No. 1 paper, and the residue was subjected to a second maceration under identical conditions. The resulting filtrates were pooled and concentrated using a rotary evaporator at temperatures between 55 to 60 °C, maintained under a vacuum pressure of 180–200 mbar. The crude extracts were combined and freeze-dried (38.3 g, 7.19% yield).

4.7. Chemicals and Reagents

Bergenin and pectolinarigenin were procured from Chengdu Alfa Biotechnology (Chengdu, China) and Wuhan ChemNorm Biotech (Wuhan, China), respectively. Specific compounds, including perforatic acid (Supplementary Figure S1), *O*-methyllaloptaeroxyrin (Supplementary Figure S2), and peucenin-7-methyl ether (Supplementary Figure S3), were isolated from the roots of *H. perforata*. Regarding the solvents and laboratory reagents, 95% commercial-grade ethanol was sourced from ITALMAR (Bangkok, Thailand), while HPLC-grade acetonitrile and AR-grade DMSO were supplied by RCI-Labscan (Bangkok, Thailand). Trifluoroacetic acid (99.9%) was obtained from Acros Organics (Antwerp, Belgium). Biological and assay-related materials, such as indomethacin, lipopolysaccharide from *E. coli* 055:B5 (LPS), and 3-(4,5-dimethylthiazol-2-yl)-2,5-diphenyltetrazolium bromide (MTT), were purchased from Sigma-Aldrich (St. Louis, MO, USA). Additionally, cell culture essentials, including fetal bovine serum (FBS), Penicillin-Streptomycin (P/S), Dulbecco's Modified Eagle's Medium (DMEM), 0.4% Trypan blue stain, and Trypsin-EDTA, were provided by Gibco (Waltham, MA, USA).

4.8. HPLC Analysis

The HPLC analysis was conducted on an Agilent 1260 Infinity II Prime HPLC system (Agilent Technologies, CA, USA). A Luna C18(2) column (5 µm, 100 Å, 250 x 4.6 mm, Phenomenex® (Phenomenex Inc. VA9525100, Torrance, CA, USA) was employed for separation, with a flow rate set at 0.8 mL/min, 20 µL, with retention times extending up to 160 min. Chromatographic analysis was carried out at a detection wavelength of 254 nm. The separation was carried out using a mobile phase comprising 0.1% (v/v) trifluoroacetic acid in aqueous solution (A) and acetonitrile (B). The gradient elution profile was programmed as follows: 2–10% B (0–30 min), 10–20% B (30–60 min), 20–30% B (60–85 min), 30–60% B (85–120 min), and 60–100% B (120–155 min), followed by a 5-minute hold. Identification of the chromatographic peaks was achieved by comparing both retention times and UV spectra with those of known reference standards, specifically bergenin, perforatic acid, *O*-methyllaloptaeroxyrin, pectolinarigenin, and peucenin-7-methyl ether. The quantity of these marker compounds within the BLW extract was subsequently determined using their corresponding calibration curves.

4.9. Nitric Oxide (NO) Inhibitory Activity and Cytotoxicity of the BLW Extract and Biomarkers on RAW 264.7 Macrophages

The RAW 264.7 murine macrophage cell line, sourced from the American Type Culture Collection (ATCC TIB-71), was maintained in Dulbecco's Modified Eagle Medium (DMEM), which was supplemented with 1% penicillin-streptomycin and 10% heat-inactivated fetal bovine serum (FBS). The cultures were incubated at 37 °C in a humidified atmosphere containing 5% CO_2.

The inhibitory effect of the BLW extract and its biomarker compounds on NO production was evaluated following an established protocol [51]. First, RAW 264.7 cells were seeded into 96-well plates at a density of 1 x 10^5 cells per well and allowed to adhere for 24 hours. Subsequently, the cells were treated simultaneously with various concentrations of the samples (1–100 µg/mL) and 1 µg/mL of LPS for a further 24-hour incubation period. To quantify NO levels, 100 µL of the culture supernatant was allowed to react with Griess reagent, and the absorbance was recorded at 520 nm.

 doi:10.20944/preprints202602.1199.v1

Indomethacin was used as a positive control, and all experiments were performed in triplicate. The percentage of NO inhibition was determined using the formula: % Inhibition = [($OD_{control}$ - OD_{sample})/$OD_{control}$] × 100, where OD_{sample}, is the optical density of the sample (treated in LPS-induced cells); $OD_{control}$, is the optical density of the solvent (treated in LPS-induced cells). Half-maximal inhibitory concentration (IC_{50}) values were obtained using GraphPad Prism software version 10.0.0 (Dotmatics, Boston, MA, USA).

Cytotoxicity of the BLW extract and its biomarker compounds against RAW 264.7 cells was assessed via the MTT colorimetric assay. After 24 hours of sample treatment, 10 µL of MTT solution (5 mg/mL in PBS) was added to each well and incubated for 2 hrs. After removal of the supernatant, 75 µL of DMSO was added to solubilize the resulting formazan crystals. The absorbance of the formazan solution was then measured using a microplate reader at 570 nm. Samples causing cell viability below 70% were considered cytotoxic [52]. Percentage cell viability was calculated as follows: cell viability (%) = (OD_{sample}) / $OD_{control}$) × 100, where OD_{sample} is the OD of the non-LPS-induced cells treated with the sample, and $OD_{control}$ is the OD of the non-LPS-induced cells treated with solvent.

4.10. Statistical Analysis

Network pharmacology data were analyzed using the bioinformatics platforms previously specified, with a *p*-value threshold of less than 0.05 defining statistical significance. All laboratory experiments regarding chemical composition and biological activity were conducted in triplicate, and the resulting data were expressed as mean ± standard deviation (SD). To ensure the validity of the parametric tests, the datasets were verified for normal distribution using the Shapiro-Wilk test and for homogeneity of variance through Levene's test. Comparative analysis between groups was performed using one-way analysis of variance (ANOVA), followed by Tukey's post-hoc test for multiple comparisons. For these analyses, a more stringent significance level was established at $p < 0.01$. All statistical analyses were carried out using SPSS software version 16.0.0 (SPSS Inc., Chicago, IL, USA).

5. Conclusions

Network pharmacology and molecular docking were used in this study to investigate the potential mechanisms underlying TF or chronic fever, focusing on BLW remedy as a therapeutic intervention. The results of this research revealed that BLW's efficacy in the treatment of TF involves a complex interplay of multiple compounds, targets, and pathways. Specifically, BLW modulates key targets, including TNF, PTGS2, STAT3, and NFKB1, through the phenylalanine, arachidonic acid, and tyrosine metabolic pathways. These targets are central to processes such as infection, inflammation, proliferation, apoptosis, and chemotherapy resistance, all of which are implicated in TF. In addition, the BLW extract also exhibited potent NO inhibitory activity in (LPS)-induced RAW264.7 macrophages with no cytotoxicity against RAW264.7 cells. The antipyretic activity of BLW through various mechanisms may be associated with the phytochemicals of the five plants constituted BLW remedy such as bergenin, perforatic acid, O-methylalloptaeroxylin, pectolinarigenin, and peucenin-7-methyl ether. These findings serve as a pharmacological foundation to provide scientific evidence for the clinical use of BLW in the treatment of TF by focusing on its anti-inflammatory actions and confirmation of previous experimental results of some genes in therapeutic targets.

Supplementary Materials: The following supporting information can be downloaded at the website of this paper posted on Preprints.org, Table S1: ADME analysis of 32 anti-inflammatory bioactive compounds in BLW; Table S2: The 495 targets associated with 15 bioactive compounds; Table S3: The targets associated with TF; Table S4: The information in topology parameters of intersection targets; Table S5: The information of top 20 signaling pathway. Figure S1: ^{1}H NMR spectrum (400 MHz, CD_3OD) of perforatic acid (**2**); Figure S2: ^{1}H NMR spectrum

 doi:10.20944/preprints202602.1199.v1

(400 MHz, CD_3OD) of *O*-methyllaloptaeroxyrin (**3**); Figure S3: ^1H NMR spectrum (400 MHz, CD_3OD) of peucenin-7-methyl ether (**5**).

Author Contributions: C.C., R.R., A.K. and S.N.; methodology, C.C., R.R., A.K. and S.N.; software, C.C. and S.N.; validation, C.C., R.R., A.K. and S.N.; formal analysis, C.C., R.R., A.K. and S.N.; investigation, C.C. and S.N.; resources, C.C. and S.N.; data curation, C.C. and S.N.; writing—original draft preparation, C.C. and S.N.; writing—review and editing, C.C., R.R., A.K. and S.N.; visualization, C.C. and S.N.; supervision, R.R., A.K. and S.N.; project administration, S.N.; funding acquisition. All authors have read and agreed to the published version of the manuscript.

Funding: The research project was financially supported by Mahasarakham University, Thailand (No. 6620919187).

Institutional Review Board Statement: Not applicable.

Informed Consent Statement: Not applicable.

Data Availability Statement: The original contributions presented in this study are included in the article/supplementary material. Further inquiries can be directed to the corresponding author(s).

Acknowledgments: The authors acknowledge the Faculty of Pharmacy, Mahasarakham University, Thailand, for funding and providing the necessary resources. A.K. thanks the FCT-Foundation for Science and Technology with the scope of UIDB/04423/2020 and UIDP/04423/2020 for support.

Conflicts of Interest: The authors declare no conflicts of interest.

Abbreviations

The following abbreviations are used in this manuscript:

BLW	Benjalokawichian
BP	Biological Process
CC	Cellular Component
GI	Gastrointestinal
GO	Gene Ontology
KEGG	Kyoto Encyclopedia of Genes and Genomes
MCODE	Molecular Complex Detection
MF	Molecular Function
NFKB1	Nuclear factor-kappa-B p105 subunit
PPI	Protein-Protein Interaction
PTGS2	Prostaglandin-Endoperoxide Synthase 2
STAT3	Signal Transducer and Activator of Transcription 3
STRING	Search Tool for the Retrieval of Interacting Genes
TF	Toxic Fever
TNF	Tumor Necrosis Factor-α
TTM	Thai Traditional Medicine

References

1. Lai, J.; Wu, H.; Qin, A. Cytokines in febrile diseases. *J. Interferon Cytokine Res.* **2021**, *41*, 1-11.
2. Ma, L.L.; Liu, H.M.; Luo, C.H.; He, Y.N.; Wang, F.; Huang, H.Z.; Han, L.; Yang, M.; Xu, R.C.; Zhang, D.K. Fever and antipyretic supported by traditional Chinese medicine: A multi-pathway regulation. *Front. Pharmacol.* **2021**, *12*, 583279.
3. Palo, T.; Thaworn, A.; Charoenkij, P.; Thamsermsang, O.; Chotewuttakorn, S.; Tripatara, P.; Laohapand, T.; Akarasereenont, P. The effects of Thai herbal Ha-Rak formula on COX isoform expression in human umbilical vein endothelial cells induced by IL-1β. *Evid. Based Complement Alternat. Med.* **2017**, *2017*, 9383272.
4. Wang, B.; Wu, L.; Chen, J.; Dong, L.; Chen, C.; Wen, Z.; Hu, J.; Fleming, I.; Wang, D.W. Metabolism pathways of arachidonic acids: Mechanisms and potential therapeutic targets. *Sig. Transduct. Target. Ther.* **2021**, *6*, 94.

 doi:10.20944/preprints202602.1199.v1

5. Tredicine, M.; Mucci, M.; Recchiuti, A.; Mattoscio, D. Immunoregulatory mechanisms of the arachidonic acid pathway in cancer. *FEBS Lett.* **2025**, *599*, 927-951.
6. Subin, P.; Sabuhom, P.; Naladta, A.; Luecha, P.; Nualkaew, S.; Nualkaew, N. An evaluation of the anti-inflammatory effects of a Thai traditional polyherbal recipe TPDM6315 in LPS-induced RAW264.7 macrophages and TNF-induced 3T3-L1 adipocytes. *Curr. Issues Mol. Biol.* **2023**, *45*, 4891-4907.
7. Balli, S.; Shumway, K.R.; Sharan, S. *Physiology, fever*. In: StatPearls [Internet], Treasure Island (FL), Eds.; StatPearls: Florida, USA, 2023. Available online: https://www.ncbi.nlm.nih.gov/books/NBK562334/ (accessed on 12 August 2024).
8. Shimizu, M. Clinical features of cytokine storm syndrome. *Adv. Exp. Med. Biol.* **2024**, *1448*, 33-42.
9. Traditional Thai Medicine Rehabilitation Foundation, Ayurveda College (Jivaka Kumar Bhaccha). Original Thai traditional medical textbook (Paetsart Sonkau): Conservation edition. 3rd ed; Printing Press of Chulalongkorn University, Bangkok, Thailand, 2015; pp. 345-356.
10. Chaloemram, C. Scientific-based explanation of Thai traditional medicine theory for Thai traditional herbal remedy (A case study of Mo-Ha-Rak formula). Doctoral dissertation, Mahasarakham University, Maha Sarakham, Thailand, January 2025.
11. National Drug Committee. List of herbal medicine products A.D. 2006. Nonthaburi: Agricultural Co-operative Federation of Thailand, Ltd., Thailand, 2006.
12. Suttana, W.; Singharachai, C.; Charoensup, R.; Rujanapun, N.; Suya, C. Antiproliferative and apoptosis-inducing activities of Benchalokawichian remedy against doxorubicin-sensitive and -resistant erythromyelogenous leukemic cells. *CMU J. Nat. Sci.* **2021**, *20*, e2021056.
13. Herbal Products Division, Food and Drug Administration. National list of essential herbal medicines 2023. Pathum Thani: Minnie Group Co., Ltd., Thailand, 2023; pp. 73-74.
14. Wang, X-H.; Li, Y-H.; Zhang, J-C.; Li, Z.; Liu, G-X.; Zhang, T.; Zhang, M-Y. Analysis of the effect of Bupleurum on fever in Xiaochaihu Decoction based on network pharmacology. *J. Hainan Med. Univ.* **2021**, *27*, 55-59.
15. Pei, K.; Wang, Y.; Guo, W.; Lin, H.; Lin, Z.; Lv, G. Antipyretic mechanism of Bai Hu Tang on LPS-induced fever in rat: A network pharmacology and metabolomics analysis. *Pharmaceuticals* **2025**, *18*, 610.
16. Zhang, H.; Ge, S.; Diao, F.; Song, W.; Zhang, Y.; Zhuang, P.; Zhang, Y. Network pharmacology integrated with experimental verification reveals the antipyretic characteristics and mechanism of Zi Xue powder. *Pharm. Biol.* **2023**, *61*, 1512–1524.
17. Zhou, W.; Zhang, H.; Wang, X.; Kang, J.; Guo, W.; Zhou, L.; Liu, H.; Wang, M.; Jia, R.; Du, X.; Wang, W.; Zhang, B.; Li, S. Network pharmacology to unveil the mechanism of Moluodan in the treatment of chronic atrophic gastritis. *Phytomedicine* **2022**, *95*, 153837.
18. Chen, W.; Li, Y.; Zhang, C.; Zhou, H.; Ma, J.; Vaishnani, D.K.; Zeng, B.; Yu, J.; Mao, H.; Zheng, J. Multi-omics and experimental validation reveal anti-HCC mechanisms of Tibetan Liwei Muxiang pill and quercetin. *Pharmaceuticals* **2025**, *18*, 900.
19. Chaloemram, C.; Rattarom, R.; Kijjoa, A.; Nualkaew, S. Integration of network pharmacology, molecular docking and in vitro nitric oxide inhibition assay to explore the mechanism of action of Thai traditional polyherbal remedy, Mo-Ha-Rak, in the treatment of prolonged fever. *Pharmaceuticals* **2025**, *18*, 1541.
20. Patel, V.R.; Saini, S.; Dwivedi, J.; Gupta, A.K.; Shrivastava, A.K.; Misra, A. Exploring the concept and scope of polyherbal formulations: A comprehensive review. *Int. J. Herb. Med.* **2025**, *13*, 9-16.
21. Dubey, S.; Dixit, A.K. Preclinical evidence of polyherbal formulations on wound healing: A systematic review on research trends and perspectives. *J. Ayurveda Integr. Med.* **2023**, *14*, 100688.
22. Sun, J.; Qi, X.; Yang, C.; Wang, S.; Jiang, J.; Wang, L.; Song, J.; Yu, B.; Sun, M. Network pharmacology, molecular docking, and in vitro experiments reveal the role and mechanism of Tanshinone IIA in colorectal cancer treatment through the PI3K/AKT Pathway. *Drug Des. Devel. Ther.* **2025**, *19*, 2959-2977.
23. Nadjar, A.; Bluthé, RM.; May, M.J.; Dantzer, R.; Parnet, P. Inactivation of the cerebral NFκB pathway inhibits interleukin-1β-induced sickness behavior and c-Fos expression in various brain nuclei. *Neuropsychopharmacol* **2005**, *30*, 1492–1499.
24. Juckmeta, T. Biological activities of the ethanolic extracts from Pikut Benjalokawichian (Ha-Rak) and its isolate compounds. Master's Thesis, Thammasat University, Bangkok, Thailand, 2011.

 doi:10.20944/preprints202602.1199.v1

25. Feng, Y.; Bhandari, R.; Li, C.; Shu, P.; Shaikh, I.I. Pectolinarigenin suppresses LPS-induced inflammatory response in macrophages and attenuates DSS-induced colitis by modulating the NF-κB/Nrf2 signaling pathway. *Inflammation* **2022**, *45*, 2529–2543.
26. Zhang, S.S.; Yang, X.; Zhang, W.X.; Zhou, Y.; Wei, T.T.; Cui, N.; Du, J.; Liu, W.; Lu, Q.B. Metabolic alterations in urine among the patients with severe fever with thrombocytopenia syndrome. *Virol. J.* **2024**, *21*, 11.
27. Luporini, R.L.; Pott-Junior, H.; Di Medeiros Leal, M.C.B.; Castro, A.; Ferreira, A.G.; Cominetti, M.R. de Freitas Anibal, F. Phenylalanine and COVID-19: Tracking disease severity markers. *Int. Immunopharmacol.* **2021**, *101*, 108313.
28. Kaewnoi, A.; Duanyai, S.; Vallisuta, O.; Yahuafai, J. Comparison of in vitro anti-inflammatory activity of extracts from original Ya-Ha-Rak and adapted formula. *J. Basic. App. Pharmacol.* **2024**, *4*, O98-O107.
29. Booranasubkajorn, S.; Kanlaya, H.; Huabprasert, S.; Lumlerdkij, N.; Akarasereenont, P.; Tripatara, P. The effect of Thai herbal Ha-Rak formula (HRF) on LPS-induced systemic inflammation in Wistar rats. *Siriraj Med. J.* **2017**, *69*, 356-362.
30. Konsue, A.; Sattayasai, J.; Puapairoj, P.; Picheansoonthon, C. Antipyretic effects of Bencha-Loga-Wichien herbal drug in rats. *Thai J. Pharmacol.* **2008**, *29*, 79-82.
31. Jongchanapong, A.; Singharachai, C.; Palanuvej, C.; Ruangrungsi, N.; Towiwat, P. Antipyretic and antinociceptive effects of Ben-Cha-Lo-Ka-Wi-Chian remedy. *J. Health Res.* **2010**, *24*, 15-22.
32. Luo, X.; Yu, Z.; Yue, B.; Ren, J.; Zhang, J.; Mani, S.; Wang, Z.; Dou, W. Obacunone reduces inflammatory signalling and tumour occurrence in mice with chronic inflammation-induced colorectal cancer. *Pharm. Biol.* **2020**, *58*, 886-897.
33. Choodej, S.; Sommit, D.; Pudhom, K. Rearranged limonoids and chromones from *Harrisonia perforata* and their anti-inflammatory activity. *Bioorg. Med. Chem. Lett.* **2013**, *23*, 3896–3900.
34. Tangsongcharoen, T.; Issaravanich, S.; Palanuvej, C.; Ruangrungsi, N. Quantitative analysis of hispidulin content in *Clerodendrum petasites* roots distributed in Thailand. *Pharmacog. J.* **2019**, *11*, 1093-1099.
35. Yu, CI.; Cheng, C.I.; Kang, Y.F.; Chang, P.C.; Lin, I.P.; Kuo, Y.H.; Jhou, A.J.; Lin, M.Y.; Chen, C.Y.; Lee, C.H. Hispidulin inhibits neuroinflammation in lipopolysaccharide-activated BV2 microglia and attenuates the activation of Akt, NF-κB, and STAT3 pathway. *Neurotox. Res.* **2020**, *38*, 163–174.
36. Jain, R.; Rawat, S.; Jain, S.C. Phytochemicals and antioxidant evaluation of *Ficus racemosa* root bark. *J. Pharm. Res.* **2013**, *6*, 615-619.
37. Boonsong, N.; Preeprame, S.; Putalun, W. Quantitative determination of bergenin in callus, twig and root of *Ficus racemosa* L. extract by high performance liquid chromatography. *KKU Res. J. (GS)* **2022**, *22*, 87-98.
38. Stitmannaitham, M, Isolation and structural determination of compounds from roots of *Harrisonia perforata* Merr. Master's Thesis, Chulalongkorn University, Bangkok, Thailand, 1992.
39. Thadaniti, S.; Archakunakorn, W.; Tuntiwachwuttikul P.; Bremner, J.B. Chromones from *Harrisonia perforata* (Blanco.) Merr. *J. Sci. Soc. Thailand* **1994**, *20*, 183-187.
40. Chunthorng-Orn, J.; Pipatrattanaseree, W.; Juckmeta, T.; Dechayont, B.; Phuaklee, P.; Itharat, A. Quality evaluation and pectolinarigenin contents analysis of Harak remedy in Thailand. *J. Health Sci. Altern. Med.* **2019**, *1*, 25-33.
41. Sakpakdeejaroen, I.; Juckmeta, T.; Itharat, A. Development and validation of RP-HPLC method to determine anti-allergic compound in Thai traditional remedy called Benjalokawichien. *J. Med. Assoc. Thai.* **2014**, *97*, S76-S80.
42. Gao, X.J.; Guo, M.Y.; Zhang, Z.C.; Wang, T.C.; Cao, Y.G.; Zhang, N.S. Bergenin plays an anti-inflammatory role via the modulation of MAPK and NF-κB signaling pathways in a mouse model of LPS-induced mastitis. *Inflammation* **2015**, *38*, 1142-50.
43. Alanazi, S.T.; Salama, S.A.; Althobaiti, M.M.; Alotaibi, R.A.; AlAbdullatif, A.A.; Musa, A.; Harisa, G.I. Alleviation of copper-induced hepatotoxicity by bergenin: Diminution of oxidative stress, inflammation, and apoptosis via targeting SIRT1/FOXO3a/NF-κB axes and p38 MAPK signaling. *Biol. Trace. Elem. Res.* **2025**, *203*, 3195-3207.

 doi:10.20944/preprints202602.1199.v1

44. Juckmeta, T.; Pipatrattanaseree, W.; Jaidee, W.; Dechayont, B.; Chunthorng-Orn, J.; Andersen, R.J.; Itharat, A. Cytotoxicity to five cancer cell lines of the respiratory tract system and anti-inflammatory activity of Thai traditional remedy. *Nat. Prod. Commun.* **2019**, *14*, 1-6.
45. Nutmakul, T.; Pattanapanyasat, K.; Soonthornchareonnon, N.; Shiomi, K.; Mori, M.; Prathanturarug, S. Antiplasmodial activities of a Thai traditional antipyretic formulation, Bencha-Loga-Wichian: A comparative study between the roots and their substitutes, the stems. *J. Ethnopharmacol*. **2016**, *193*, 125-132.
46. Chuchote, C.; Somwong, P. Similarity analysis of the chromatographic fingerprints of Thai herbal Ya-Ha-Rak remedy using HPLC. *Interprof. J. Health Sci.* **2019**, *17*, 55-63.
47. Somwong, P.; Chuchote, C. Determination of lupeol, a cytotoxic compound against SW620 cells in the extracts of Ha-Rak recipe. *Pharmacogn J.* **2021**, *13*, 133-138.
48. Ryszkiewicz, P.; Schlicker, E.; Malinowska, B. Is inducible nitric oxide synthase (iNOS) promising as a new target against pulmonary hypertension?. *Antioxidants* **2025**, *14*, 377.
49. Soufli, I.; Toumi, R.; Rafa, H.; Touil-Boukoffa, C. Overview of cytokines and nitric oxide involvement in immuno-pathogenesis of inflammatory bowel diseases. *World J. Gastrointest. Pharmacol. Ther.* **2016**, *7*, 353-360.
50. Pal, P.P.; Begum, A.S.; Basha, S.A.; Araya, H.; Fujimoto, Y. New natural pro-inflammatory cytokines (TNF-α, IL-6 and IL-1β) and iNOS inhibitors identified from *Penicillium polonicum* through in vitro and in vivo studies. *Int. Immunopharmacol.* **2023**, *117*, 109940.
51. Pratama, R.R.; Sari, R.A.; Sholikhah, I.; Mansor, H.; Chang, H-I.; Sukardiman.; Widyowati, R. Inhibition of nitric oxide production in RAW 264.7 cells and cytokines IL-1β in osteoarthritis rat models of 70% ethanol extract of *Arcangelisia flava* (L.) merr stems. *Heliyon* **2024**, *10*, e35730.
52. Juckmeta, T.; Itharat, A. Anti-inflammatory and antioxidant activities of Thai traditional remedy called "Ya-ha-rak". *J. Health Res*. **2012**, *26*, 205-210.
53. Chandranipapongse, W.; Palo, T.; Chotewuttakorn, S.; Tripatara, P.; Booranasubkajorn, S.; Laohapand, T.; Akarasereenont, P. Study the effect of an antipyretic drug, Thai herbal Ha-Rak formula on platelet aggregation in healthy Thai volunteers: A randomized, placebo-controlled trial. *Siriraj Med. J.* **2017**, *69*, 283-289.
54. Daina, A.; Michielin, O.; Zoete, V. SwissADME: A free web tool to evaluate pharmacokinetics, drug-likeness and medicinal chemistry friendliness of small molecules. *Sci. Rep.* **2017**, *7*, 42717.
55. Kim, S.; Thiessen, P.A.; Bolton, E.E.; Chen, J.; Fu, G.; Gindulyte, A.; Han, L.; He, J.; He, S.; Shoemaker, B.A.; Wang, J.; Yu, B.; Zhang, J.; Bryant, S.H. PubChem substance and compound databases. *Nucleic Acids Res*. **2016**, *44*, D1202–D1213.
56. Gfeller, D.; Grosdidier, A.; Wirth, W.; Daina, A.; Michielin, O.; Zoete, V. Swisstarget prediction: a web server for target prediction of bioactive small molecules. *Nucleic Acids Res*. **2014**, *42*, W32–W38.
57. Safran, M.; Dalah, I.; Alexander, J.; Rosen, N.; Stein, T.I.; Shmoish, M.; Nativ, N.; Bahir, I.; Doniger, T.; Krug, H.; Sirota-Madi, A.; Olender, T.; Golan, Y.; Stelzer, G.; Harel, A.; Lancet, D. GeneCards version 3: The human gene integrator. *Database (Oxford)* **2010**, *2010*, baq020.
58. Amberger, J.S.; Bocchini, C.A.; Schiettecatte, F.; Scott, A.F.; Hamosh, A. OMIM.org: Online mendelian inheritance in man (OMIM®), an online catalog of human genes and genetic disorders. *Nucleic Acids Res.* **2015**, *43*, D789–D798.
59. Whirl-Carrillo, M.; McDonagh, E.M.; Hebert, J.M.; Gong, L.; Sangkuhl, K.; Thorn, C.F.; Altman, R.B.; Klein, T.E. An evidence-based framework for evaluating pharmacogenomics knowledge for personalized medicine. *Clin. Pharm. Therap*. **2021**, *92*, 414–417.
60. Szklarczyk, D.; Gable, A.L.; Lyon, D.; Junge, A.; Wyder, S.; Huerta-Cepas, J.; Simonovic, M.; Doncheva, N.T.; Morris, J.H.; Bork, P.; Jensen, E.J.; von Mering, C. STRING v11: Protein-protein association networks with increased coverage, supporting functional discovery in genome-wide experimental datasets. *Nucleic Acids Res*. **2019**, *47*, D607–D613.
61. Sherman, B.T.; Hao, M.; Qiu, J.; Jiao, X.; Baseler, M.W.; Lane, H.C.; Imamichi, T.; Chang, W. DAVID: A web server for functional enrichment analysis and functional annotation of gene lists (2021 update). *Nucleic Acids Res*. **2022**, *50*, W216–W221.

 doi:10.20944/preprints202602.1199.v1

62. Salman, H.A.; Yaakop, A.S.; Aladaileh, S.; Mustafa, M.; Gharaibeh, M.; Kahar, U.M. Inhibitory effects of *Ephedra alte* on IL-6, hybrid TLR4, TNF-α, IL-1β, and extracted TLR4 receptors: In silico molecular docking. *Heliyon* **2023**, *9*, e12730.
63. Shrivastava, N.; Joshi, J.; Sehgal, N.; Kumar, I.P. Cyclooxygenase-2 identified as a potential target for novel radiomodulator scopolamine methyl bromide: An in silico study. *Inform. Med. Unlocked* **2017**, *9*, 18–25.
64. Liu, W.; Chu, Z.; Yang, C.; Yang, Y.; Wu, H.; Sun, J. Discovery of potent STAT3 inhibitors using structure-based virtual screening, molecular dynamic simulation, and biological evaluation. *Front. Oncol.* **2023**, *13*, 1287797.
65. Piccagli, L.; Fabbri, E.; Borgatti, M.; Bezzerri, V.; Mancini, I.; Nicolis, E.; Dechecchi, M.C.; Lampronti, I.; Cabrini, G.; Gambari, R. Docking of molecules identified in bioactive medicinal plants extracts into the p50 NF-kappaB transcription factor: Correlation with inhibition of NF-kappaB/DNA interactions and inhibitory effects on IL-8 gene expression. *BMC Struct. Biol.* **2008**, *8*, 38.
66. Trott, O.; Olson, A.J. AutoDock Vina: Improving the speed and accuracy of docking with a new scoring function, efficient optimization and multithreading. *J. Comput. Chem.* **2010**, *31*, 455–461.
67. Shivaleela, B.; Srushti, S.C.; Shreedevi, S.J.; Babu, R.L. Thalidomide-based inhibitor for TNF-α: Designing and in silico evaluation. *Futur. J. Pharm. Sci.* **2022**, *8*, 5
68. Antoniou, K.; Malamas, M.; Drosos, A.A. Clinical pharmacology of celecoxib, a COX-2 selective inhibitor. *Expert Opin. Pharmacother.* **2007**, *8*, 1719–1732.
69. Miyoshi, K.; Takaishi, M.; Nakajima, K.; Ikeda, M.; Kanda, T.; Tarutani, M.; Iiyama, T.; Asao, N.; DiGiovanni, J.; Sano, S. STAT3 as a therapeutic target for the treatment of psoriasis: A clinical feasibility study with STA-21, a STAT3 inhibitor. *J. Invest. Dermatol*. **2011**, *131*, 108-17.
70. Kashyap, T.; Argueta, C.; Aboukameel, A.; Unger, T.J.; Klebanov, B.; Mohammad, R.M.; Muqbil, I.; Azmi, A.S.; Drolen, C.; Senapedis, W.; Lee, M.; Kauffman, M.; Shacham, S.; Landesman, Y. Selinexor, a selective inhibitor of nuclear export (SINE) compound, acts through NF-κB deactivation and combines with proteasome inhibitors to synergistically induce tumor cell death. *Oncotarget*. **2016**, *7*, 78883-78895.